

## MIT Open Access Articles

*Consumption of atmospheric hydrogen during  
the life cycle of soil-dwelling actinobacteria*

The MIT Faculty has made this article openly available. **Please share**  
how this access benefits you. Your story matters.

**Citation:** Meredith, Laura K., Deepa Rao, Tanja Bosak, Vanja Klepac-Ceraj, Kendall R. Tada, Colleen M. Hansel, Shuhei Ono, and Ronald G. Prinn. "Consumption of Atmospheric Hydrogen During the Life Cycle of Soil-Dwelling Actinobacteria." *Environmental Microbiology Reports* 6, no. 3 (November 20, 2013): 226–238.

**As Published:** <http://dx.doi.org/10.1111/1758-2229.12116>

**Publisher:** Wiley Blackwell

**Persistent URL:** <http://hdl.handle.net/1721.1/99163>

**Version:** Author's final manuscript: final author's manuscript post peer review, without publisher's formatting or copy editing

**Terms of use:** Creative Commons Attribution-Noncommercial-Share Alike



**Title Page**

**Title:** Consumption of atmospheric H<sub>2</sub> during the life cycle of soil-dwelling actinobacteria

**Authors:** Laura K. Meredith<sup>1,4</sup>, Deepa Rao<sup>1,5</sup>, Tanja Bosak<sup>1</sup>, Vanja Klepac-Ceraj<sup>2</sup>, Kendall R. Tada<sup>2</sup>, Colleen M. Hansel<sup>3</sup>, Shuhei Ono<sup>1</sup>, and Ronald G. Prinn<sup>1</sup>

(1) Massachusetts Institute of Technology, Department of Earth, Atmospheric and Planetary Science, Cambridge, Massachusetts, 02139, USA.

(2) Wellesley College, Department of Biological Sciences, Wellesley, Massachusetts, 02481, USA.

(3) Woods Hole Oceanographic Institution, Department of Marine Chemistry and Geochemistry, Woods Hole, Massachusetts, 02543, USA.

**Corresponding author:**

Laura K. Meredith

Address: 77 Massachusetts Ave., 54-1320, Cambridge, MA, 02139

Telephone: (617) 253-2321

Fax: (617) 253-0354

Email: [predawn@mit.edu](mailto:predawn@mit.edu)

**Running title:** Uptake of H<sub>2</sub> during the life cycle of soil actinobacteria

**Summary**

Microbe-mediated soil uptake is the largest and most uncertain variable in the budget of atmospheric hydrogen (H<sub>2</sub>). The diversity and ecophysiological role of soil microorganisms that can consume low atmospheric abundances of H<sub>2</sub> with high-affinity [NiFe]-hydrogenases is

**Author current addresses:** (4) Stanford University, Environmental Earth System Science, Palo Alto, CA, 94305, USA. (5) Georgetown University, Communication, Culture and Technology, Washington, DC, 20057.

22 unknown. We expanded the library of atmospheric H<sub>2</sub>-consuming strains to include four soil  
23 Harvard Forest Isolate (HFI) *Streptomyces* spp., *Streptomyces cattleya*, and *Rhodococcus equi* by  
24 assaying for high-affinity hydrogenase (*hhyL*) genes and quantifying H<sub>2</sub> uptake rates. We find  
25 that aerial structures (hyphae and spores) are important for *Streptomyces* H<sub>2</sub> consumption; uptake  
26 was not observed in *Streptomyces griseoflavus* Tu4000 (deficient in aerial structures) and was  
27 reduced by physical disruption of *Streptomyces* sp. HFI8 aerial structures. H<sub>2</sub> consumption  
28 depended on the life cycle stage in developmentally distinct actinobacteria: *Streptomyces* sp.  
29 HFI8 (sporulating) and *R. equi* (non-sporulating, non-filamentous). Strain HFI8 took up H<sub>2</sub> only  
30 after forming aerial hyphae and sporulating, while *R. equi* only consumed H<sub>2</sub> in the late  
31 exponential and stationary phase. These observations suggest that conditions favoring H<sub>2</sub> uptake  
32 by actinobacteria are associated with energy and nutrient limitation. Thus, H<sub>2</sub> may be an  
33 important energy source for soil microorganisms inhabiting systems in which nutrients are  
34 frequently limited.

## 35 Main Text

### 36 Introduction

37 Microbe-mediated soil uptake is the leading driver of variability in atmospheric H<sub>2</sub> and accounts  
38 for 60% to 90% of the total H<sub>2</sub> sink; however, the dependence of this sink on environmental  
39 parameters is poorly constrained by field and lab measurements (Xiao et al., 2007; recently  
40 reviewed by Ehhalt and Rohrer, 2009). Atmospheric H<sub>2</sub> is an abundant reduced trace gas (global  
41 average of 530 ppb) that influences the atmospheric chemistry of the troposphere and the  
42 protective stratospheric ozone layer (Novelli et al., 1999). Most notably, the reaction of H<sub>2</sub> with  
43 the hydroxyl radical ( $\bullet\text{OH}$ ) attenuates the amount of  $\bullet\text{OH}$  available to scavenge potent  
44 greenhouse gases, like methane (CH<sub>4</sub>), from the atmosphere. The H<sub>2</sub> soil sink may play a

45 considerable role in buffering anthropogenic H<sub>2</sub> emissions, which constitute approximately 50%  
46 of atmospheric H<sub>2</sub> sources (Ehhalt and Rohrer, 2009). A process-level understanding of the H<sub>2</sub>  
47 soil sink is required to understand the natural variability of atmospheric H<sub>2</sub> and its sensitivity to  
48 changes in climate and anthropogenic activities.

49 Early studies established the H<sub>2</sub> soil sink as a biological process because of the enzymatic  
50 nature of H<sub>2</sub> consumption (Conrad and Seiler, 1981; Schuler and Conrad, 1990; Häring and  
51 Conrad, 1994). Initially, free soil hydrogenases were thought to be the primary drivers of the H<sub>2</sub>  
52 soil sink because chemical fumigation of soils had little effect on soil H<sub>2</sub> uptake rates but  
53 significantly reduced the active microbial consumption or production of other trace gases, *e.g.*,  
54 the active microbial uptake of CO (Conrad and Seiler, 1981; Conrad et al., 1983b; Conrad,  
55 1996). Only indirect evidence existed to support the notion that the soil sink was an active  
56 microbial process (Conrad and Seiler, 1981; Conrad et al. 1983a; King, 2003b) until the isolation  
57 of *Streptomyces* sp. PCB7, the first microorganism to exhibit significant consumption of  
58 atmospheric H<sub>2</sub> (Constant et al., 2008). This organism demonstrated high-affinity ( $K_m \sim 10\text{-}50$   
59 ppm), low-threshold ( $< 0.1$  ppm) H<sub>2</sub> uptake kinetics characteristic of uptake by environmental  
60 soil samples (Conrad, 1996). Previously, only low-affinity ( $K_m \sim 1000$  ppm), high-threshold ( $>$   
61 0.5 ppm) H<sub>2</sub>-oxidizing microorganisms were characterized, which were unable to consume H<sub>2</sub> at  
62 atmospheric concentrations (Conrad et al., 1983b; Conrad, 1996; Guo and Conrad, 2008;  
63 summarized by Constant et al., 2009).

64 *Streptomyces* spp. are ubiquitous soil microorganisms that degrade recalcitrant materials  
65 in soils (Kieser et al., 2000). Theoretically, the observed rates of atmospheric H<sub>2</sub> soil  
66 consumption can sustain the maintenance energy requirements for typical numbers of  
67 *Streptomyces* spp. cells in soils (Conrad, 1999; Constant et al., 2010; Constant et al., 2011a).

68 However, the importance of atmospheric H<sub>2</sub> as a source of energy to soil microorganisms  
69 remains unknown. Atmospheric H<sub>2</sub> uptake was specifically linked to a group 5 [NiFe]-  
70 hydrogenase gene cluster containing genes that encode for the small and large hydrogenase  
71 subunits, *hhyS* and *hhyL*, respectively (Constant et al., 2010). The *hhyL* gene is distributed  
72 unevenly amongst the Actinobacteria, Proteobacteria, Chloroflexi, and Acidobacteria phyla (*e.g.*,  
73 many, but not all *Streptomyces* spp. possess the gene) (Constant et al., 2010; Constant et al.,  
74 2011b). The link between high-affinity H<sub>2</sub> uptake and *hhyL* has been reported in nine  
75 *Streptomyces* spp. and in *Mycobacterium smegmatis* (Constant et al., 2011b; King, 2003b), but it  
76 remains untested in many soil microorganisms. Additional research adding to the library of  
77 atmospheric H<sub>2</sub>-oxidizing bacteria is needed to identify the key microorganisms involved in H<sub>2</sub>  
78 biogeochemical cycling. Information about the genes and ecophysiology of these organisms can  
79 improve the process-level understanding of the H<sub>2</sub> soil sink (Conrad, 1996; Madsen, 2005).

80         The life cycle of *Streptomyces* is complex and controls the timing of many physiological  
81 activities, which may include H<sub>2</sub> uptake (Kieser et al., 2000; Schrempf, 2008; Flärdh and  
82 Buttner, 2009). In soils, *Streptomyces* exist predominantly as inactive spores, which germinate in  
83 response to environmental triggers such as moisture and nutrient availability (Kieser et al., 2000)  
84 and grow vegetatively, producing a network of mycelia that grow into the substrate (Flärdh and  
85 Buttner, 2009). Over time, and in response to environmental triggers such as nutrient depletion  
86 or physiological stresses, the colony differentiates to form hydrophobic aerial hyphae that break  
87 the substrate surface tension and grow into the air, forming a millimeter-scale canopy in  
88 immediate contact with the atmosphere (Kieser et al., 2000; Schrempf, 2008). Finally, aerial  
89 hyphae differentiate and septate to form chains of resistant spores (Flärdh and Buttner, 2009). In  
90 cultures of *Streptomyces* sp. PCB7 growing on soil particles, H<sub>2</sub> uptake coincided with the

91 presence of aerial hyphae and spores (Constant et al., 2008). It is unknown if H<sub>2</sub> uptake occurs at  
92 the same life cycle stage in other *Streptomyces* strains and how long uptake persists in the spore  
93 stage. Furthermore, the timing of atmospheric H<sub>2</sub> uptake in microbes that possess *hhyL*, but do  
94 not sporulate has not been measured.

95         The goal of this paper is to address two questions. First, our study asks whether  
96 environmental isolates and culture collection strains with the genetic potential for atmospheric  
97 H<sub>2</sub> uptake, i.e., the *hhyL* gene, actually exhibit atmospheric H<sub>2</sub> uptake. To expand the library of  
98 atmospheric H<sub>2</sub>-oxidizing bacteria, we quantify H<sub>2</sub> uptake rates by novel *Streptomyces* soil  
99 isolates that contain the *hhyL* and by three previously isolated and sequenced strains of  
100 actinobacteria whose *hhyL* sequences span the known *hhyL* diversity. Second, we investigate  
101 how H<sub>2</sub> uptake varies over organismal life cycle in one sporulating and one non-sporulating  
102 microorganism, *Streptomyces* sp. HFI8 and *Rhodococcus equi*, respectively. These experiments  
103 probe the advantage of atmospheric H<sub>2</sub> consumption to microbes and relationship between  
104 environmental conditions, physiology of soil microbes, and H<sub>2</sub>.

## 105 **Results**

### 106         **H<sub>2</sub> uptake by microbial soil isolates and culture collection strains possessing *hhyL*.**

107         Candidate *Streptomyces* strains, referred to henceforth as Harvard Forest Isolate (HFI)  
108 strains, were isolated from Harvard Forest soils. PCR amplification revealed that *hhyL* encoding  
109 the high-affinity [NiFe]-hydrogenase was present in six out of nine tested strains. Four of these  
110 strains (HFI6, HFI7, HFI8, and HFI9) were successfully retained in culture and were used to test  
111 the link between *hhyL* and H<sub>2</sub> uptake activity. These strains exhibited distinctive *Streptomyces*  
112 traits such as pigmentation, a fuzzy appearance indicating the production of aerial hyphae  
113 (Figures S1 and S2), and the distinctive earthy scent of geosmin (Schrempf, 2008). The 16S

114 rRNA gene sequences of the new isolates fell within the *Streptomyces* genus and were 100%  
115 identical to several different strains of *Streptomyces* spp. (Table S1). Of two clusters that were  
116 defined by Constant et al. (2011b) based on a deeply rooted split (99% of bootstrap replicates) in  
117 the phylogenetic tree of *hhyL* amino acid sequences (Figure S3), the HFI6 - HFI9 *hhyL*  
118 sequences group with *hhyL* Cluster 1. In addition to our *Streptomyces* isolates, we examined  
119 three culture collection strains in this study to broaden representation across the *hhyL* clusters  
120 and genera (Bergey et al., 1957): *Streptomyces griseoflavus* Tu4000 (Cluster 1), *Rhodococcus*  
121 *equi* (Actinobacterium, Cluster 1), and *Streptomyces cattleya* (Cluster 2).

122 (Insert Table 1 here)

123 To test whether organisms with *hhyL* gene sequences consume H<sub>2</sub>, we measured the  
124 uptake of atmospheric H<sub>2</sub> in sporulated *Streptomyces* cultures and in stationary stage of *R. equi*.  
125 The presence of *hhyL* predicted atmospheric H<sub>2</sub> uptake activity in HFI strains 6-9, *S. cattleya*,  
126 and *R. equi*, but not in *S. griseoflavus* Tu4000 (Table 1). We find that atmospheric H<sub>2</sub> uptake  
127 observed in strains with *hhyL* from Cluster 1 (*Streptomyces* strains HFI6 - HFI9 and *R. equi*) and  
128 Cluster 2 (*S. cattleya*). The biomass-weighted H<sub>2</sub> uptake rates of these isolates spanned nearly  
129 two orders of magnitude (from 10 to 780 nmol min<sup>-1</sup> g<sup>-1</sup>), and the *Streptomyces* strains that took  
130 up H<sub>2</sub> did so at rates more than 10-fold greater than dense stationary phase cultures of *R. equi*  
131 (Table 1). *R. equi* consumed atmospheric H<sub>2</sub>, both when grown on solid R2A medium and in  
132 liquid TSB medium (data not shown). Uptake rates of *Streptomyces* cultures were measured on  
133 solid medium because *Streptomyces* cultures typically do not progress through their full  
134 developmental cycle in liquid medium (Flärdh and Buttner, 2009). The Michaelis-Menten  
135 substrate affinity was determined from the x-intercept of Lineweaver-Burk plots of the inverse  
136 relationship between the first-order H<sub>2</sub> uptake rate and initial headspace H<sub>2</sub> concentrations

137 between 0 and 35 ppm. This method can be more error prone than the non-inverse approach  
138 performed over a greater range of initial H<sub>2</sub> mole fractions, but it better restricts H<sub>2</sub> uptake by  
139 low-affinity hydrogenases, and has enough sensitivity to distinguish high- and low-affinity  
140 uptake kinetics. K<sub>m</sub> values of HFI strains were typically low (40-80 ppm for HFI strains), which  
141 indicated that enzymatic processing of H<sub>2</sub> is tuned to operate efficiently at atmospheric levels of  
142 H<sub>2</sub> (high-affinity uptake). *S. cattleya* and *R. equi* appeared have high- or intermediate-affinity K<sub>m</sub>  
143 values (<1000 ppm), but did not pass the quality control measures (Experimental Procedures) to  
144 be included in Table 1. The minimum H<sub>2</sub> concentration, or threshold, consumed by each HFI  
145 strain ranged from 0.12 to 0.15 ppm, which is well below typical atmospheric mole fractions of  
146 around 0.53 ppm (Table 1). *S. cattleya* and *R. equi* thresholds were also below atmospheric  
147 levels at least below 0.45 and 0.30 ppm, respectively (Table 1). This study augments the library  
148 of organisms that contain *hhyL* sequences and take up atmospheric H<sub>2</sub> with high-affinity and a  
149 low-threshold from 10 to 16 strains.

### 150 **H<sub>2</sub> uptake correlates with lifecycle stage in *Streptomyces* sp. HFI8**

151 We randomly selected *Streptomyces* sp. HFI8 from our HFI strains as a representative  
152 organism to determine whether high-affinity H<sub>2</sub> consumption depended on the stage of the life  
153 cycle and how long uptake lasted in the sporulation stage. Microscopy revealed the progression  
154 of strain HFI8 through developmental stages over 44 days on solid agar (Figure S4). Following  
155 germination, the colonies of strain HFI8 grew as substrate mycelia (Figure S4-A). By day 1.8 the  
156 lawn reached its maximal aerial coverage and grew upward as aerial hyphae formed and then  
157 sporulated (Figure S4-B). The co-occurrence of partially septated aerial hyphae and spores  
158 indicated that the events were not simultaneous throughout the colony (Figure S4-B).  
159 Measurements of H<sub>2</sub> uptake revealed that H<sub>2</sub> consumption began only after the formation of



160 aerial hyphae and sporulation around day 2 (Figure 1). Aerial hyphae formation and sporulation  
161 are stages of the life cycle often associated with nutrient limitation in *Streptomyces* spp. H<sub>2</sub>  
162 uptake reached a maximum rate (9.4±2.3 nmol h<sup>-1</sup>) on day 3.8, two days after sporulation had  
163 begun, and then slowly decreased over the next 40 days, dropping below the detection limit of  
164 ±0.24 nmol h<sup>-1</sup>. Most cells between days 2.9 and 44 were a lawn of “dormant” spores that had  
165 completed the full life cycle (Figures S4-C-H). H<sub>2</sub> oxidation rates by dormant spores declined  
166 slowly over the 44-day experiment to negligible rates (Figure 1). All three replicates displayed  
167 similar timing, but the H<sub>2</sub> uptake rates were systematically lower in the third replicate, although  
168 the area coverage of the lawn and biomass was not demonstrably different among the replicates.  
169 A cursory set of measurements (data not shown) indicated similar trends in H<sub>2</sub> uptake over the  
170 life cycle of *Streptomyces* sp. HFI6, *Streptomyces* sp. HFI7, *Streptomyces* sp. HFI9, and *S.*  
171 *cattleya*.

172 (Insert Table 2 here)

173 Because the formation of aerial biomass (hyphae and spores) occurred at the same time as  
174 the onset of H<sub>2</sub> consumption in *Streptomyces*, we asked whether H<sub>2</sub> uptake activity was  
175 physically located in the aerial biomass. We isolated the aerial fraction (spores and aerial  
176 hyphae) of strain HFI8 cultures by gently rolling glass beads over the entire surface of the colony  
177 and transferring the beads and aerial biomass to an empty, sterile glass vial (Figure S5). H<sub>2</sub>  
178 uptake rates were measured in whole cultures before the transfer, in the vials with the transferred  
179 aerial fraction, and in the original vial with the substrate fraction that remained after the glass  
180 bead procedure (Table 2, Samples 1-6; Figure S5). The experiment lasted 2-4 hours following  
181 the aerial biomass transfer. H<sub>2</sub> uptake in the transferred aerial biomass fraction was consistently  
182 low, typically near or below the limit of detection of ±0.24 nmol h<sup>-1</sup>, and was thus often

183 statistically indistinguishable from zero. Low uptake rates in the aerial fraction were not the  
184 result of poor biomass transfer efficiency by the glass bead procedure; glass beads transferred a  
185 significant proportion (Table 2,  $0.7\pm 0.6$  mg) of the aerial biomass from the replicate cultures of  
186 that could be collected using a metal spatula ( $1.2\pm 0.5$  mg). The drop in uptake also cannot be  
187 explained by aging over this period, because this occurs over the course of days or weeks and not  
188 hours (Figure 1). No reduction in H<sub>2</sub> uptake stemming from reduced spore viability was expected  
189 because the biomass transfer procedure by glass beads is based on established methods for  
190 harvesting viable spores (*e.g.*, Hirsch and Ensign, 1976; Hardisson et al., 1978). Furthermore, the  
191 number of viable spores in bead-treated cultures was indistinguishable from the number of viable  
192 spores obtained by transferring aerial biomass by a metal spatula from replicate vials incubated  
193 at the same time. This test was done by harvesting spores by the two methods, plating spore  
194 suspension dilutions, and counting the number of colony forming units as a function of the initial  
195 amount of biomass (protein mass) in the spore suspensions.

196 We found that the net H<sub>2</sub> uptake diminished after the separation of the aerial biomass  
197 from the substrate biomass (Table 2). Even in replicates where glass beads were gently rolled  
198 over strain HFI8 lawns and all biomass was left in the original vial, net H<sub>2</sub> uptake was  
199 significantly reduced (Table 2, Samples 7-12). The larger the initial H<sub>2</sub> oxidation rate, the larger  
200 percentage reduction by the glass beads (Figure S6, linear fit,  $R^2=0.93$ ), regardless of culture age  
201 or the amount of glass beads used for transfer (Samples 1-12). These experiments suggested that  
202 the colony structure and the presence of intact aerial hyphae were important for H<sub>2</sub> uptake.

203 **H<sub>2</sub> uptake correlates with the growth stage of *Rhodococcus equi***

204 (Insert Figure 2 here)

205           Only some microbes containing *hhyL* are sporulating *Streptomyces* (Figure S3). To test  
206 whether H<sub>2</sub> uptake by non-sporulating Actinobacterium *R. equi* is related to its lifecycle, we  
207 measured the uptake of H<sub>2</sub> by this organism at various stages of growth in liquid cultures (Figure  
208 2). The growth phases were determined from optical density measurements of the cultures. *R.*  
209 *equi* did not consume measurable quantities of H<sub>2</sub> during the exponential growth phase (day 1 to  
210 4), but started taking up H<sub>2</sub> in the late exponential growth phase (day 4 to 7) and in the stationary  
211 phase (day 7 to 17) until the end of the experiment (Figure 2). The late exponential phase and  
212 stationary phase growth stages are associated with nutrient limitation.

213           The low H<sub>2</sub> uptake rates by *R. equi* were much closer to the experimental detection limit  
214 than *Streptomyces* sp. HFI8. This suggested that the lack of uptake could be related to low *R.*  
215 *equi* cell densities in late exponential and early stationary phase rather the altered cell  
216 physiology. To test this, we concentrated cells from a culture in exponential growth phase (day  
217 1.9) into either fresh medium or sterile water to match the cell densities (Figure 2b) of H<sub>2</sub>-  
218 oxidizing cultures in the late exponential and early stationary phases (comparable to those on  
219 days 4-6). In spite of the comparable cell densities, cells concentrated in this manner did not  
220 consume H<sub>2</sub> ( $-0.075 \pm 0.15$  nmol h<sup>-1</sup>, Figure 2a). In addition, we diluted cells in stationary phase  
221 (day 7.8) into fresh medium or water to obtain suspensions whose cell densities matched those  
222 during days 2-3 of the exponential phase (Figure 2). Although H<sub>2</sub> oxidation rates of the  
223 exponentially growing cultures on days 2 and 3 were below the limit of detection ( $\pm 0.12$  nmol h<sup>-1</sup>),  
224 comparably dense cells derived from the diluted stationary phase cultures took up H<sub>2</sub>  
225 ( $0.43 \pm 0.047$  nmol h<sup>-1</sup>). All cultures were shaken vigorously to ensure the delivery of H<sub>2</sub> into the  
226 medium. Some extracellular factors of relevance to H<sub>2</sub> uptake, such as extracellular  
227 hydrogenases, may have been carried over into the diluted suspensions. The decrease in the

228 uptake of H<sub>2</sub> by stationary phase cells (74% of undiluted uptake) did not scale with the dilution  
229 (22% of the undiluted cell biomass), which corresponds to a relative mismatch factor of 3.5 in H<sub>2</sub>  
230 uptake versus dilution. The reason is unclear, and could result from H<sub>2</sub> substrate diffusion  
231 limitation in very dense cultures, which was partially alleviated upon dilution. If the cultures  
232 were diffusion limited for H<sub>2</sub> substrate, the observed H<sub>2</sub> oxidation rate (Table 1) and H<sub>2</sub> uptake  
233 rates during late exponential and stationary phases (Figure 2) may underestimate the potential H<sub>2</sub>  
234 uptake by cultures of *R. equi*. The uptake of H<sub>2</sub> only by stationary phase cells, either in the old  
235 culture medium or when resuspended in fresh medium or water, related the uptake of H<sub>2</sub> to the  
236 late exponential and stationary phases. Overall, these tests linked *R. equi* H<sub>2</sub> consumption with  
237 growth phase.

## 238 **Discussion**

### 239 **Link between *hhyL* and H<sub>2</sub> uptake**

240 Our results confirm links between *hhyL* and H<sub>2</sub> uptake to include *R. equi*, four  
241 *Streptomyces* HFI soil isolates from Cluster 1, and *S. cattleya* from Cluster 2, thereby providing  
242 additional support for the use of the high-affinity hydrogenase gene *hhyL* as a predictor for the  
243 capability to consume atmospheric hydrogen. H<sub>2</sub> uptake by *hhyL* by strains from Clusters 1 and 2  
244 indicate that the phylogenetic divergence between the two groups does not compromise  
245 atmospheric H<sub>2</sub> uptake activity by *hhyL*, or its prediction. Strains HFI6 - HFI9 exhibit high H<sub>2</sub>  
246 uptake affinities and low uptake thresholds. Culture collection strains exhibit more variable H<sub>2</sub>  
247 uptake kinetics, in keeping with a recent suggestion that H<sub>2</sub> consuming microorganisms exhibit a  
248 continuum of affinities rather than a discrete grouping of high and low affinities (Constant et al.,  
249 2010). Current observations of high-affinity H<sub>2</sub> uptake are limited to the *Actinobacteria*, and  
250 future studies are required to determine whether H<sub>2</sub> uptake occurs in the other phyla containing

251 the *hhyL* gene, such as Chloroflexi, Planctomycetes, Verrucomicrobia, and Proteobacteria  
252 (Figure S3). A genome data-mining investigation revealed the ubiquity of *hhyL* in DNA  
253 extracted from forest, desert, agricultural, and peat soils samples, and although some evidence  
254 suggests a correlation between soil H<sub>2</sub> uptake rates and the number of H<sub>2</sub>-oxidizing bacteria, no  
255 correlation was found between *hhyL* DNA copies and soil H<sub>2</sub> uptake rates (Constant et al.,  
256 2011a; Constant et al., 2011b). Future work should be aimed both at understanding the diversity  
257 and ecophysiology of these *hhyL*-containing microorganisms and at developing methods to  
258 predict H<sub>2</sub> uptake activity across ecosystems.

### 259 **H<sub>2</sub> uptake and the developmental cycle of actinobacteria**

260 Our results support a correlation between the developmental stage of *Streptomyces* spp.  
261 and high-affinity H<sub>2</sub> uptake in two ways. First, we did not observe any H<sub>2</sub> uptake in the substrate  
262 mycelium developmental phase of *Streptomyces* sp. HFI8. H<sub>2</sub> uptake began only after the  
263 formation of aerial hyphae and sporulation. Second, we found that *S. griseoflavus* Tu4000, which  
264 grew predominantly as substrate mycelium, did not take up H<sub>2</sub>. We propose that the impaired  
265 development (i.e. lack of aerial hyphae and/or spores) of *S. griseoflavus* Tu4000 may impair the  
266 production or activity of its high-affinity hydrogenase. In culture, *S. griseoflavus* Tu4000 is  
267 smooth and waxy, and does not produce the aerial hyphae typical of *Streptomyces* grown on  
268 solid culture (Figure S1 and S2). *S. griseoflavus* Tu4000 may belong to a class of *bld* (bald)  
269 mutants that are often deficient in aerial hyphae production (Kieser et al., 2000). Sporulation  
270 efficiency is also often reduced in *bld* mutants (Szabó and Vitalis, 1992), and *S. griseoflavus*  
271 Tu4000 does not form spores on various types of media (J. Blodgett, personal communication),  
272 including our cultures. To our knowledge, *S. griseoflavus* Tu4000 is the first *hhyL*-containing  
273 *Streptomyces* sp. found to be unable to oxidize atmospheric H<sub>2</sub> under the same experimental

274 conditions that lead to H<sub>2</sub> oxidation by other *Streptomyces* spp. High-affinity H<sub>2</sub> uptake is also  
275 absent from Cluster 1 *hhyL* containing cultures of a gram-negative beta-proteobacterium  
276 *Ralstonia eutropha* H16 (formerly known as *Alcaligenes eutropha* 16) grown on solid medium  
277 and tested for uptake in suspensions (Conrad et al., 1983b). Future experiments could compare  
278 sporulating *Streptomyces* with their *bld* mutants or stimulate the formation of aerial hyphae  
279 and/or sporulation in *bld Streptomyces* spp. mutants by application of exogenous  $\delta$ -butyrolactone  
280 factor (Ueda et al., 2000; Straight and Kolter, 2009), and determine the effect of this stimulation  
281 on H<sub>2</sub> oxidation or *hhyL* expression. In summary, the combined lack of aerial hyphae, spores,  
282 and H<sub>2</sub> uptake in *S. griseoflavus* Tu4000 and the co-occurrence of these phenotypes in strain  
283 HFI8 underscored a strong developmental control of atmospheric H<sub>2</sub> uptake in *Streptomyces*.  
284 These observations motivate the use of *Streptomyces* mutants arrested at different points in the  
285 developmental cycle to investigate the regulation and physiological role of *hhyL* in sporulating  
286 actinobacteria.

287         Our measurements of H<sub>2</sub> uptake in HFI8 colonies disturbed by glass beads indicate that  
288 H<sub>2</sub> uptake depends on the physical structure of *Streptomyces* aggregates. Cultures treated by  
289 glass beads take up less H<sub>2</sub>, suggesting that the activity of the hydrogenase is impaired by the  
290 disturbance of the aerial structures. H<sub>2</sub> uptake by the disrupted colony could decrease because of  
291 loss in structural support, loss in signaling and nutrient transport within the bacterial lawn  
292 (Miguélez et al., 1999), or reduction in the aerial hyphae surface area in contact with the air.  
293 Therefore, we attribute the observed decrease in H<sub>2</sub> uptake to physical destruction of the lawn  
294 and colony structure of *Streptomyces*.

295         The H<sub>2</sub> uptake by non-sporulating batch cultures of *R. equi* occurs only during late  
296 exponential and stationary phase, suggesting that its H<sub>2</sub> consumption may support metabolism

297 under nutrient-limiting conditions. Similarly, H<sub>2</sub> uptake by strain HFI8 is present only during  
298 those stages of its life cycle associated with nutrient-limiting conditions, suggesting that H<sub>2</sub> may  
299 be an important energy source for *Streptomyces* under stress. This is consistent with previous  
300 reports of H<sub>2</sub> oxidation by *M. smegmatis*, a non-sporulating Actinobacterium with a Cluster 1  
301 high-affinity [NiFe]-hydrogenase that can persist for many years in host tissue in a nutrient-  
302 deprived stationary phase (Smeulders et al, 1999; King, 2003b). *M. smegmatis* expresses the  
303 hydrogenase gene under starvation conditions and mutants lacking this hydrogenase have a  
304 reduced growth yield under these conditions (Berney and Cook, 2010). Therefore, the ability to  
305 scavenge low concentrations of H<sub>2</sub> may be an important adaptation of various sporulating and  
306 non-sporulating actinobacteria (Prescott, 1991; Smeulders et al, 1999; Scherr and Nguyen,  
307 2009). This could be particularly true in terrestrial environments where nutrient concentrations are  
308 often low for extended periods and atmospheric H<sub>2</sub> is available.

### 309 **Implications for soil H<sub>2</sub> uptake in the environment**

310 Uptake of atmospheric H<sub>2</sub> by spores, which are often considered to be metabolically  
311 dormant, may have consequences for both the sporulating microbes and the cycling of H<sub>2</sub> in the  
312 environment. H<sub>2</sub> oxidation rates in cultures of strain HFI8 continue to increase for two days after  
313 the onset of sporulation. This could reflect heterogeneity in the sample, because not all cells  
314 sporulate simultaneously, or maximum H<sub>2</sub> uptake by already formed spores. In any case,  
315 measurable H<sub>2</sub> oxidation in sporulated cultures persists for over a month, such that the time-  
316 integrated H<sub>2</sub> oxidation in any culture is much larger in spore state than at any other stage in the  
317 life cycle. Net H<sub>2</sub> consumption by HFI8 is at least tenfold larger in the spore state (days 4-44)  
318 than during the growth of substrate mycelium (through day 1.1) and formation of aerial hyphae  
319 (after day 1.8) combined. One should also keep in mind that the H<sub>2</sub> uptake rates measured in

320 culture studies depend on the specific medium, and may not be directly translated to different  
321 media or soil types, where the nutritional characteristics, moisture levels, and cell abundances  
322 likely differ. The persistence of H<sub>2</sub> oxidation by *Streptomyces* spp. may have consequences for  
323 environmental H<sub>2</sub> cycling and environmental conditions that promote the removal of atmospheric  
324 H<sub>2</sub>. Conditions that favor germination and growth, including soil moisture and nutrient  
325 availability (Kieser et al., 2000), may increase the population of *Streptomyces* spp. in the  
326 substrate mycelium phase and actually limit the amount of H<sub>2</sub> oxidized by soils. During  
327 moisture- or nutrient-limiting conditions, a greater fraction of the population of *Streptomyces*  
328 spp. will be in life cycle stages linked with H<sub>2</sub> uptake (aerial hyphae and spores).  
329 Counterintuitively, H<sub>2</sub> uptake by *Streptomyces* spp. may be most significant when the  
330 environmental conditions are the harshest. H<sub>2</sub> uptake in spores under our experimental conditions  
331 is reduced to negligible levels after about a month (Figure 1), indicating that H<sub>2</sub> uptake may be  
332 very low in environments where conditions are harsh for long periods, such as deserts.

333         Ultimately, the goal of studying microbial influences on trace gas fluxes is to understand  
334 and predict emergent biogeochemical cycling in the environment. This study describes H<sub>2</sub>  
335 consumption by two developmentally distinct actinobacteria under nutrient-limiting conditions.  
336 Field measurements along a chronosequence of recent volcanic deposits support this notion by  
337 suggesting that relative uptake of H<sub>2</sub> by the soil microbial community (normalized by soil  
338 respiration rates) is most important when soils were limited by organic carbon (King, 2003a).  
339 However, insignificant or even opposing trends also exist (Conrad and Seiler, 1985; Rahn et al.,  
340 2002), which may be driven by other factors. Future studies are also needed to determine the  
341 impact of nutrient- and moisture-limiting conditions on H<sub>2</sub> uptake by soils and to consider the  
342 significance and implications of the energetic supply from H<sub>2</sub> for the microorganisms in the



343 competitive soil environment. A better understanding of the process-level controls on microbe-  
344 mediated H<sub>2</sub> soil uptake is critical for evaluating the impact of a changing climate on the soil H<sub>2</sub>  
345 uptake and the impact of continued anthropogenic H<sub>2</sub> emissions on atmospheric chemistry and  
346 climate.

347

## 348 **Experimental Procedures**

### 349 **Microbial Strains**

350 *Streptomyces* spp. were isolated from soils within the footprint of the Environmental  
351 Measurement Site (EMS) atmospheric trace gas flux tower at the Harvard Forest Long Term  
352 Ecological Research site in Petersham, MA (42°32'N, 72°11'W). Atmospheric H<sub>2</sub> fluxes were  
353 concurrently measured at the same site (Meredith, 2012). Harvard Forest is a mixed deciduous  
354 forest with acidic soils originating from sandy loam glacial till (Allen, 1995). Most H<sub>2</sub>  
355 consumption occurs within the first few centimeters of soil beneath the litter layer (Yonemura et  
356 al., 2000; Smith-Downey et al., 2008); therefore, samples were collected from the uppermost six  
357 inches of soil after removal of the leaf litter. Sporulating soil organisms such as *Streptomyces*  
358 spp. were enriched for using desiccation and chemical destruction (El-Nakeeb and Lechavalier,  
359 1963; Schrempf, 2008). Soils were dried for 3-4 hours at 55°C. Dry soil samples (1 g) were  
360 ground with a mortar and pestle and were combined with CaCO<sub>3</sub> (1 g). The soil mixtures were  
361 incubated for 2 days at 28°C in 100x15 mm polystyrene Petri dishes (sterile, polystyrene,  
362 100x15 mm, VWR, Radnor, PA), with moistened filter paper (11.0 cm diameter, Grade 1,  
363 Whatman®, Kent, ME) fitted in the lids to maintain a humid environment. After this period,  
364 incubated soil mixtures were suspended in 100 ml sterile water and thoroughly vortexed. After

365 settling for 30 min, soil suspensions were serially diluted, and the  $10^0$ ,  $10^{-2}$ , and  $10^{-4}$  dilutions  
366 were spread onto R2A plates (Difco™ R2A, BD, Franklin Lakes, NJ) that had been treated with  
367 88 mg cycloheximide / L medium (Porter et al., 1960). After incubation at 30°C for 3-5 days,  
368 microbial colonies were screened for the presence of any of the following four distinctive  
369 *Streptomyces* traits: 1) antibiotic inhibition of neighboring growth (*i.e.*, zone of clearing), 2) a  
370 fuzzy appearance indicating the production of aerial hyphae (Figures S1 and S2), 3)  
371 pigmentation, or 4) the distinctive earthy scent of geosmin (Schrempf, 2008). Those exhibiting  
372 any of the traits were serially transferred onto fresh R2A plates until pure isolates were obtained.  
373 The resulting set of isolates, henceforth referred to as Harvard Forest Isolates (HFI), was  
374 maintained in culture on R2A agar at room temperature. Strains HFI6, HFI7, HFI8, and HFI9  
375 were deposited to the United States Department of Agriculture NRRL Culture Collection for  
376 preservation as NRRL B-24941, NRRL B-24943, NRRL B-24942, and NRRL B-24940,  
377 respectively.

378         Strains from culture collections that were used in this study have published genomes  
379 accessible in the National Center for Biotechnology Information (NCBI) databases  
380 (<http://www.ncbi.nlm.nih.gov/>). *Streptomyces griseoflavus* Tu4000 (accession NZ GG657758)  
381 was kindly provided by the genome authors and collaborators (Michael Fischbach, John Clardy,  
382 Joshua Blodgett). The following strains were obtained from culture collections: *Rhodococcus*  
383 *equi* ATCC 33707™ (accession CM001149) and *Streptomyces cattleya* NRRL 8057 (accession  
384 NC 016111).

### 385         **DNA extraction and PCR amplification**

386         DNA was extracted using the PowerSoil® DNA Extraction Kit (MoBio Laboratories,  
387 Carlsbad, CA) from colonies. PCR amplification of 16S rRNA and *hhyL* genes, respectively, was

388 performed using a Mastercycler<sup>®</sup> pro (Eppendorf, Hamburg, Germany) in 25 µl reaction volumes  
389 with the following reaction mixture: 12.125 µl ddH<sub>2</sub>O, 1.25 µl BSA (Roche, Indianapolis, IN),  
390 2.5 µl 10x Ex Taq Buffer (TaKaRa), 0.125 (5 units/ µl) Ex Taq (TaKaRa), 2 µl dNTP (2.5 mM  
391 TaKaRa), 2.5 µl of each primer suspended at 3µM (IDT, Coralville, IA). The 16S rRNA gene  
392 was amplified using universal primers 27F:5'-AGA GTT TGA TCC TGG CTC AG-3' and  
393 1492R:5'-ACG GCT ACC TTG TTA CGA CTT-3' (Lane, 1991), and *hhyL* gene was amplified  
394 using NiFe244F:5' - GGG ATC TGC GGG GAC AAC CA -3' and NiFe-1640R:5'-TGC ACG  
395 GCG TCC TCG TAC GG -3' (Constant et al., 2010). The following program was used: 5 min  
396 initial denaturation at 95°C, followed by 30 cycles consisting of 30 s template denaturation at  
397 95°C, 30 s hold at the primer annealing temperature, 1.5 min extension at 72°C, and a final  
398 extension at 72°C for 5 min. Annealing temperatures of 50°C and 60.7°C were used for the  
399 amplification of the 16S rRNA and *hhyL* genes, respectively. The *hhyL* annealing temperature  
400 was optimized over a temperature gradient spanning eight temperatures between 50°C and  
401 62.2°C using *S. griseoflavus* Tu4000 DNA as template.

402 Each HFI strain was evaluated for the presence of a putative group 5 [NiFe]-hydrogenase  
403 by gel electrophoresis of the *hhyL* gene PCR reaction product. Gels were cast (1% agarose, 5µl  
404 GelRed nucleic acid stain (Biotum, Hayward, CA)), loaded (5µl PCR product and 2µl DNA  
405 loading dye (Fermentas, Glen Burnie, MD)), run (100 V for 1 hr), and visualized (UVP  
406 MultiDoc-It<sup>™</sup> Digital Imaging System (UVP, Upland, CA)) to verify successful PCR  
407 amplification. Migration of HFI strain PCR product was compared to the *S. griseoflavus* Tu4000  
408 *hhyL* gene as a positive control and to the DNA Molecular Weight Marker X (Roche,  
409 Indianapolis, IN) ladder for reference.

410 **Gene sequencing and sequence analysis**

411 PCR products were sequenced at Genewiz (Cambridge, MA) following the  
412 manufacturer's sample preparation guidelines. Both 16S rRNA and *hhyL* gene sequences  
413 (trimmed for >Q30) were identified by BLASTN (Altschul et al., 1990) and listed in Table  
414 S1. Hydrogenase *hhyL* amino acid sequences were aligned using ClustalW (Larkin et al., 2007)  
415 and phylogenetic analyses were carried out in Mega 5.2 (Tamura et al., 2011). Relationships  
416 were determined using a Maximum Likelihood method based on the Whelan and Goldman  
417 model (Whelan and Goldman, 2001) and checked for consistency using parsimony. The *hhyL*  
418 gene from archaeon *Sulfolobus islandicus* HVE10/4 was used as an outgroup. A 100 bootstrap  
419 maximum likelihood tree was constructed using Mega 5.2.

420 The gene sequences obtained for strains HFI6, HFI7, HFI8, and HFI9 were deposited in  
421 GenBank under accession numbers KC661265, KC661266, KF444073, and KF444074 for the  
422 16S rRNA genes and under accession numbers KC661267, KC661268, KC661269, and  
423 KC661270 for the *hhyL* genes. 16S rRNA gene sequences were compared with published  
424 sequences in the National Center for Biotechnology Information (NCBI) gene databases  
425 (BLASTN, <http://blast.ncbi.nlm.nih.gov>) for phylogenetic identification (Table S1).

#### 426 **H<sub>2</sub> uptake assays**

427 H<sub>2</sub> oxidation rates were determined routinely by measuring the decrease in H<sub>2</sub> mole  
428 fractions in the microbial culture headspace over time. Microbial strains were cultivated  
429 aerobically on solid (R2A) or liquid (TSB) medium inside 160 ml glass serum vials. H<sub>2</sub> uptake  
430 rate measurements were initiated by isolating the serum vial headspace from the atmosphere with  
431 a crimped stopper and vials were slightly pressurized after closure by adding 15 ml of sterile lab  
432 air. Liquid cultures were continuously agitated at 200 rpm during the H<sub>2</sub> uptake assay to facilitate  
433 gas exchange across the air-liquid interface. The change in headspace H<sub>2</sub> was measured three

434 times at approximately forty-minute intervals. H<sub>2</sub> uptake followed apparent first-order kinetics  
435 over the small range (0.1 to 4 ppm) of laboratory atmospheric H<sub>2</sub> mole fractions:  $H_2(t) =$   
436  $H_2(0)e^{-bt}$ . First-order rate constants were determined from the slope (-b) of the logarithmic  
437 decrease in the headspace H<sub>2</sub> mole fraction. H<sub>2</sub> oxidation rates are reported at a H<sub>2</sub> mole fraction  
438 of 530 ppb, the estimated global mean (Novelli et al., 1999).

439 H<sub>2</sub> mole fractions were measured using a Gas Chromatograph (GC, Model 2014,  
440 Shimadzu Co., Kyoto, Japan) retrofitted with a Helium ionization Pulsed Discharge Detector  
441 (HePDD, D-4-I-SH17-R Model, Valco Instruments Co. Inc., Houston, Texas). The instrument is  
442 similar to a recently described system for measuring H<sub>2</sub> at atmospheric levels (approximately  
443 530 ppb) and has an improved precision, linearity and stability compared to methods that use a  
444 mercuric oxide detector (Novelli et al., 2009). Details of the instrument design and performance  
445 are publically accessible in Meredith (2012). Stainless steel flasks containing compressed air  
446 were used as working standards with ambient H<sub>2</sub> mole fractions. These were calibrated using the  
447 GC-HePDD system against a tertiary standard (514.3 ppb H<sub>2</sub> in air, aluminum 150A tank,  
448 Airgas, Radnor, PA) tied to the NOAA CMD/ESRL H<sub>2</sub> scale. Precisions, assessed by repeated  
449 standard measurements, were typically <1% (1 sigma) on the Shimadzu GC-HePDD.

450 The precision for H<sub>2</sub> oxidation rate measurements is taken as two times the standard  
451 deviation of measurements of the H<sub>2</sub> uptake in sterile control vials containing the same (liquid or  
452 solid) medium as the culture vials. This precision serves as the effective detection limit, that is,  
453 the minimum H<sub>2</sub> oxidation rate that is distinguishable from zero by the measurement. Detection  
454 limits were determined separately for the time series of H<sub>2</sub> uptake rates measured in control vials  
455 for strain HFI8 and *R. equi* because of the difference in medium, and were between ( $\pm 0.12$  and

456  $\pm 0.24 \text{ nmol h}^{-1}$ ).  $\text{H}_2$  uptake thresholds were determined after allowing the cultures to take up  $\text{H}_2$   
457 mole fractions for at least 90 minutes until headspace  $\text{H}_2$  mole fractions reached stable values.

458 The Michaelis-Menten substrate affinity ( $K_m$ ) describes the affinity of  $\text{H}_2$  uptake, relevant  
459 to the broad range of  $\text{H}_2$  concentrations that occur in soils ( $\text{H}_2$  mole fractions ranging from 0.01  
460 to 1000 ppm) (Schink, 1997; Constant et al., 2008). Kinetic parameters of  $\text{H}_2$  uptake were  
461 determined in sporulated *Streptomyces* cultures and in the stationary phase cultures of *R. equi*.  
462 The dependency of  $\text{H}_2$  uptake rates on initial  $\text{H}_2$  mole fractions were determined over a range of  
463 initial headspace  $\text{H}_2$  mole fractions (set at about eight levels between 0.5 and 35 ppm  $\text{H}_2$  by  
464 injecting a 1%  $\text{H}_2$  in  $\text{N}_2$  mix into the sealed headspace). Headspace  $\text{H}_2$  was measured twice, 15  
465 minutes apart in each culture containing different initial  $\text{H}_2$  concentrations, and  $\text{H}_2$  uptake was  
466 calculated from the linear uptake rate. The  $K_m$  and the maximum reaction rate ( $V_{\max}$ ) for each  
467 strain was determined from Lineweaver-Burk (LB) plots of the inverse of the uptake rate ( $1/V$ )  
468 versus the inverse of the substrate concentration ( $1/S$ ) the initial  $\text{H}_2$  mole fraction.  $K_m$  was  
469 determined as the  $K_m = -1 / x$ -intercept and  $V_{\max}$  as  $V_{\max} = 1/y$ -intercept (Constant et al., 2008).  
470 As a crosscheck for the quality of the reported kinetic parameters, Eadie-Hofstee (EH) plots of  $V$   
471 versus  $V/S$  were used to determine  $K_m$  from  $K_m = -\text{slope}$ .  $K_m$  and  $V_{\max}$  values were reported for a  
472 given strain only if the LB and EH  $K_m$  values methods agreed within 50%. A typical LB and EH  
473 plot is shown in Figure S7.  $\text{H}_2$  uptake thresholds were determined after allowing the cultures to  
474 take up  $\text{H}_2$  mole fractions for at least 90 minutes until headspace  $\text{H}_2$  mole fractions reached  
475 stable values.

#### 476 **Lifecycle analysis of *Streptomyces* spp.**

477 The life cycle of *Streptomyces* spp. cultures was tracked in parallel with the  $\text{H}_2$  uptake to  
478 test the influence of developmental stage on atmospheric  $\text{H}_2$  uptake. Serum vials (160 mL)

479 containing 10 ml of R2A medium were inoculated with 100  $\mu$ l of the spore suspension onto the  
480 agar surface. Control vials were supplemented with 100  $\mu$ l sterile H<sub>2</sub>O. The developmental stages  
481 were assessed by microscopy, using a Zeiss Axio Imager.M1 microscope and Axio Cam MRm  
482 camera using Axio Vision (4.8) software (Zeiss, Peabody, MA).

483 Growth rates of filamentous organisms grown on solid media are difficult to measure;  
484 instead, photographs of the fractional area covered by *Streptomyces* colonies in the serum vial  
485 were used as an indication of growth rate. Final aerial biomass was quantified by a protein assay.  
486 Aerial biomass was aseptically harvested using a metal spatula and transferred to 1.5 ml tubes  
487 containing 0.3 g of glass beads (0.2 mm diameter) and 0.7 ml water. Cells were vortexed for 5  
488 min at 2000 rpm followed by cooling on ice and then sonicated with three 30 s bursts and 1 min  
489 intermittent cooling on ice. Residues of membranes and nucleic acids were removed by  
490 transferring 0.5 ml of the protein extract to Costar<sup>®</sup> Spin-X<sup>®</sup> microcentrifuge filter tubes  
491 (Corning, Inc., Corning, NY) and centrifuging at 10,000 rpm for 15 minutes. Protein  
492 concentrations were determined using the Pierce BCA protein assay kit (Thermo Scientific,  
493 Rockford, IL) and a Synergy 2 Microplate Reader (BioTek, Winooski, VT) controlled by Gen5  
494 (1.04.5) software.

495 To determine whether H<sub>2</sub> uptake in the aerial fraction (containing hyphae and spores) of a  
496 *Streptomyces* culture would continue to take up H<sub>2</sub> when separated from the substrate mycelium  
497 and medium, H<sub>2</sub> uptake rates were measured before and after by gently rolling between 2.5 and  
498 10 g of 4 mm glass beads (Table 2) over *Streptomyces* sp. HFI8 lawns of various ages (2-15  
499 days). The lawns grew on R2A solid medium in a serum vial and the aerial biomass was  
500 transferred to a sterile glass serum vial containing no medium (Figure S5). H<sub>2</sub> uptake rates were  
501 measured in the original culture vial, the lawn was treated with the glass beads and aerial

502 biomass was transferred immediately by moving the glass beads to a sterile vial. H<sub>2</sub> uptake rates  
503 were measured over the next 2-4 h in the sterile vial containing the isolated aerial biomass on  
504 glass beads, and in the original vial containing medium and the remaining substrate mycelium.  
505 The amount of biomass that was transferred was quantified using the protein assay described  
506 above. This procedure was performed for six replicates at different time points after sporulation  
507 and with different amounts of glass beads (Table 2, Samples 1-6). In addition, the effect of the  
508 glass beads on H<sub>2</sub> uptake in the absence of transfer was tested in six control samples. These  
509 samples were treated with the glass beads, but the beads remained in the original vials (Table 2,  
510 Samples 7-12) and H<sub>2</sub> uptake rates were measured in the same vials before and after disruption  
511 by glass beads.

#### 512 **Growth phase analysis of *R. equi***

513 The relationship between the growth phase and H<sub>2</sub> uptake of *R. equi* was assessed in  
514 liquid cultures. *R. equi* was inoculated by adding 100 µl of a cell suspension into 20 ml sterile  
515 TSB (Bacto™ Tryptic soy broth, BD) liquid medium in 160 ml glass serum vials. All cultures  
516 were incubated at 30°C and shaken at 200 rpm. Growth was monitored by measuring the optical  
517 density (OD) of *R. equi* cultures as the absorbance at 600 nm at 25°C in the Synergy 2  
518 Microplate Reader. The relationship between OD and protein concentration was established by  
519 constructing a calibration curve between OD measurements of serial dilutions with known  
520 protein concentrations. *R. equi* protein concentrations were determined using the same general  
521 procedure as described for the *Streptomyces* spp. The growth phase in *R. equi* cultures were  
522 established using the semilogarithmic plot of the growth curve (Figure 2), where the exponential  
523 growth phase is taken as the period with the maximum, sustained positive slope. Late  
524 exponential phase was defined as the time when the growth rate slowed down, as identified by a



525 decreasing slope of the growth curve. Finally, stationary phase occurred where the growth curve  
526 slope was zero.

527  $H_2$  uptake by *R. equi* was low. A concentration/dilution experiment was performed to test  
528 whether the negligible  $H_2$  oxidation rates at low cell densities in early exponential growth phase  
529 were the result of a lack of  $H_2$  oxidation activity or the low signal-to-noise ratio due to the small  
530 number of active cells. *R. equi* cultures were inoculated at the beginning of the experiment,  
531 concentrated in exponential phase on day 1.9 by centrifugation at 8000 rpm for 10 min, and re-  
532 suspended into either fresh TSB or in sterile  $H_2O$  to final densities of 160 and 110- $\mu\text{g protein ml}^{-1}$   
533 <sup>1</sup> in TSB and  $H_2O$ , respectively. This was within the range of densities observed in late  
534 exponential and stationary phases (100-230  $\mu\text{g protein ml}^{-1}$ ). Additionally, a sample was taken  
535 on day 7.8 in stationary phase (at a density of 190  $\mu\text{g protein ml}^{-1}$ ) and was diluted in TSB or  
536 sterile  $H_2O$  to cellular densities of 45 and 38  $\mu\text{g protein ml}^{-1}$  respectively, to match the density in  
537 the early exponential phase (10-100  $\mu\text{g protein ml}^{-1}$ ). For both the concentration and dilution  
538 experiments, the cell pellets resulting from centrifugation were not washed during the procedure  
539 so that some extracellular material and original culture medium (< 1 ml) was diluted into fresh  
540 TSB or  $H_2O$  to a maximum final concentration of 1/5<sup>th</sup>.  $H_2$  uptake rates in the headspace of the  
541 concentrated or diluted samples were measured as described above.

#### 542 **Acknowledgements**

543 The authors are grateful to Paula Welander for advice in the lab and to Diane Ivy for  
544 assistance with measurements. Strain *Streptomyces griseoflavus* Tu4000 was kindly contributed  
545 to this study by genome authors Michael Fischbach and John Clardy via Joshua Blodgett. L.K.M.  
546 is grateful for the opportunity to attend the MBL Microbial Diversity Course. L.K.M. was  
547 supported by from the following funding sources: NSF Graduate Research Fellowship, multiple

548 grants from NASA to MIT for the Advanced Global Atmospheric Gases Experiment (AGAGE),  
549 MIT Center for Global Change Science, MIT Joint Program on the Science and Policy of Global  
550 Change, MIT Martin Family Society of Fellows for Sustainability, MIT Ally of Nature Research  
551 Fund, MIT William Otis Crosby Lectureship, and MIT Warren Klein Fund. D. R. was funded  
552 through MIT Undergraduate Research Opportunities Program (UROP) with support from the  
553 Lord Foundation and Jordan J. Baruch Fund (1947) and was supported by the Harvard Forest  
554 REU Program.

555

#### 556 **Conflict of Interest**

557 Authors and co-authors have no conflicts of interest to declare.

558

#### 559 **References**

- 560 Allen, A. (1995) Soil science and survey at Harvard Forest. *Soil Surv Horiz* 36
- 561 Altschul,S.F., Gish W., Miller, W., Myers, E.W., Lipman, D.J. (1990) Basic Local Alignment  
562 Search Tool. *J Mol Biol* 215: 403–410.
- 563 Bergey, D.H. and Gibbons, N.E. (1957) *Bergey’s manual of determinative bacteriology*, 7th  
564 edn. Baltimore, USA: Williams & Wilkins Company.
- 565 Berney, M. and Cook, G.M. (2010) Unique flexibility in energy metabolism allows  
566 *mycobacteria* to combat starvation and hypoxia. *PloS ONE* 5: e8614.
- 567 Conrad, R and Seiler, W. (1981) Decomposition of atmospheric hydrogen by soil  
568 microorganisms and soil enzymes. *Soil Biol Biochem* 13: 43–49.

- 569 Conrad, R. and Seiler, W. (1985) Influence of temperature, moisture, and organic carbon on the  
570 flux of H<sub>2</sub> and CO between soil and atmosphere: field studies in subtropical regions. J  
571 Geophys Res 90: 5699–5709.
- 572 Conrad, R., Aragno, M., and Seiler, W. (1983a) Production and consumption of hydrogen in a  
573 eutrophic lake. Appl Environ Microbiol 45: 502-510.
- 574 Conrad, R., Aragno, M., and Seiler, W. (1983b) The inability of hydrogen bacteria to utilize  
575 atmospheric hydrogen is due to threshold and affinity for hydrogen. FEMS Microbiol  
576 Lett 18: 207–210.
- 577 Conrad, R. (1996) Soil microorganisms as controllers of atmospheric trace gases (H<sub>2</sub>, CO, CH<sub>4</sub>,  
578 OCS, N<sub>2</sub>O, and NO). Microbiol Rev 60: 609–640.
- 579 Conrad, R. (1999) Soil microorganisms oxidizing atmospheric trace gases (CH<sub>4</sub>, CO, H<sub>2</sub>, NO).  
580 Ind J Microbiol 39: 193–203.
- 581 Constant, P., Poissant, L., and Villemur, R. (2008) Isolation of *Streptomyces* sp. PCB7, the first  
582 microorganism demonstrating high-affinity uptake of tropospheric H<sub>2</sub>. ISME J 2: 1066–  
583 1076.
- 584 Constant, P., Poissant, L., and Villemur, R. (2009) Tropospheric H<sub>2</sub> budget and the response of  
585 its soil uptake under the changing environment. Sci Total Environ 407: 1809–1823.
- 586 Constant, P., Chowdhury, S.P., Pratscher, J., and Conrad, R. (2010) *Streptomyces* contributing  
587 to atmospheric molecular hydrogen soil uptake are widespread and encode a putative  
588 high-affinity [NiFe]-hydrogenase. Env Microbiol 12: 821–829.
- 589 Constant, P., Chowdhury, S.P., Hesse, L., and Conrad, R. (2011a) Co-localization of atmospheric  
590 H<sub>2</sub> oxidation activity and high affinity H<sub>2</sub>-oxidizing bacteria in non-axenic soil and sterile  
591 soil amended with *Streptomyces* sp. PCB7. Soil Biol Biochem 43: 1888–1893.

- 592 Constant, P., Chowdhury, S.P., Hesse, L., Pratscher, J., and Conrad, R. (2011b) Genome data  
593 mining and soil survey for the novel group 5 [NiFe]-hydrogenase to explore the diversity  
594 and ecological importance of presumptive high affinity H<sub>2</sub>-oxidizing bacteria. *Appl*  
595 *Environ Microb* 77: 6027–6035.
- 596 Ehhalt, D.H. and Rohrer, F. (2009) The tropospheric cycle of H<sub>2</sub>: a critical review. *Tellus B* 61:  
597 500–535.
- 598 El-Nakeeb, M.A. and Lechevalier, H.A. (1963) Selective isolation of aerobic Actinomycetes.  
599 *Appl Microbiol* 11: 75–77.
- 600 Flårdh, K. and Buttner, M.J. (2009) *Streptomyces* morphogenetics: dissecting differentiation in a  
601 filamentous bacterium. *Nat Rev Microbiol* 7: 36–49.
- 602 Guo, R. and Conrad, R. (2008) Extraction and characterization of soil hydrogenases oxidizing  
603 atmospheric hydrogen. *Soil Biol Biochem* 40: 1149–1154.
- 604 Häring, V. and Conrad, R. (1994) Demonstration of two different H<sub>2</sub>-oxidizing activities in soil  
605 using an H<sub>2</sub> consumption and a tritium exchange assay. *Biol Fert Soils* 17: 125–128.
- 606 Hardisson, C., Manzanal, M.B., Salas, J.A., and Suarez, J.E. (1978) Fine structure, physiology  
607 and biochemistry of arthrospore germination in *Streptomyces antibioticus*. *J. Gen.*  
608 *Microbiol.* 105: 203–214.
- 609 Hirsch, C.F. and Ensign, J.C. (1976) Nutritionally defined conditions for germination of  
610 *Streptomyces viridochromogenes* spores. *J. Bacteriol.* 126: 13–23.
- 611 Kieser, T., Bibb, M.J., Buttner, M.J., Chater, K.F., and Hopwood, D.A. (2000) Practical  
612 *Streptomyces* genetics. Norwich, UK: John Innes Foundation.
- 613 King, G.M. (2003a) Contributions of atmospheric CO and hydrogen uptake to microbial  
614 dynamics on recent Hawaiian volcanic deposits. *Appl Environ Microb* 69: 4067–4075.

- 615 King, G.M. (2003b) Uptake of carbon monoxide and hydrogen at environmentally relevant  
616 concentrations by mycobacteria. *Appl Env Microbiol* 69: 7266–7272.
- 617 Lane DJ (1991) 16S/23S rRNA sequencing. In *Nucleic acid techniques in bacterial systematics*.  
618 Stackebrandt, E. and Goodfellow, M. (eds). John Wiley and Sons, New York, pp. 115-  
619 148.
- 620 Larkin, M. A., Blackshields, G., Brown, N. P., Chenna, R., McGettigan, P. A., McWilliam, H.,  
621 Valentin, F., Wallace, I. M., Wilm, A., Lopez, R., Thompson, J.D., Gibson, T.J., and  
622 Higgins, D. G. (2007) Clustal W and Clustal X version 2.0. *Bioinformatics* (Oxford,  
623 England) 23: 2947–8.
- 624 Madsen, E.L. (2005) Identifying microorganisms responsible for ecologically significant  
625 biogeochemical processes. *Nat Rev Micro* 3: 439–446.
- 626 Meredith, L.K. (2012) Field Measurement of the Fate of Atmospheric H<sub>2</sub> in a Forest  
627 Environment: from Canopy to Soil. Doctor of philosophy thesis, Massachusetts Institute  
628 of Technology, MIT Center for Global Change Science, 250 pp.  
629 (<http://globalchange.mit.edu/research/publications/2366>)
- 630 Miguélez, E.M., Hardisson, C., and Manzanal, M. (1999) Hyphal death during colony  
631 development in *Streptomyces antibioticus*: morphological evidence for the existence of a  
632 process of cell deletion in a multicellular prokaryote. *J Cell Biol* 145: 515–525.
- 633 Novelli, P.C., Lang, P.M., Masarie, K.A., Hurst, D.F., Myers, R., Elkins, J.W. (1999) Molecular  
634 hydrogen in the troposphere: Global distribution and budget. *J Geophys Res* 104: 30,427–  
635 30,444.

- 636 Novelli, P.C., Crotwell, A.M., and Hall, B.D. (2009) Application of gas chromatography with a  
637 pulsed discharge helium ionization detector for measurements of molecular hydrogen in  
638 the atmosphere. *Environ Sci Technol* 43: 2431–2436.
- 639 Porter, J.N., Wilhelm, J.J., and Tresner, H.D. (1960) Method for the preferential isolation of  
640 Actinomycetes from soils. *Appl Microbiol* 8: 174-178.
- 641 Prescott, J.F. (1991) *Rhodococcus equi*: an animal and human pathogen. *Clin Microbiol Rev* 4:  
642 20–34.
- 643 Rahn, T., Eiler, J. M., Kitchen, N., Fessenden, J. E., and Randerson, J. T. (2002) Concentration  
644 and  $\delta D$  of molecular hydrogen in boreal forests: Ecosystem-scale systematics of  
645 atmospheric H<sub>2</sub>. *Geophys Res Lett* 29: 1–4.
- 646 Scherr, N. and Nguyen, L. (2009) *Mycobacterium* versus *Streptomyces* - we are different, we are  
647 the same. *Curr Opin Microbiol* 12: 699–707.
- 648 Schink, B. (1997) Energetics of syntrophic cooperation in methanogenic degradation. *Microbiol*  
649 *Mol Biol Rev* 61: 262-280.
- 650 Schrempf, H. (2008) Streptomycetaceae: life style, genome, metabolism and habitats.  
651 *Encyclopedia of Life Sciences*. Chichester, UK: John Wiley & Sons, pp 1–7.
- 652 Schuler, S. and Conrad, R. (1990) Soils contain two different activities for oxidation of  
653 hydrogen. *FEMS Microbiol Ecol* 73: 77–83.
- 654 Smeulders, M.J., Keer, J., Speight, R.A., and Williams, H.D. (1999) Adaptation of  
655 *Mycobacterium smegmatis* to stationary phase. *J Bacteriol* 181: 270-283.
- 656 Smith-Downey, N.V., Randerson, J.T., and Eiler, J.M. (2008) Molecular hydrogen uptake by  
657 soils in forest, desert, and marsh ecosystems in California. *J Geophys Res* 113: 1–11.

- 658 Straight, P.D. and Kolter, R. (2009) Interspecies chemical communication in bacterial  
659 development. *Ann Rev Microbiol* 63: 99–118.
- 660 Szabó, G. and Vitalis, S. (1992) Sporulation without aerial mycelium formation on agar medium  
661 by *Streptomyces bikiniensis* HH1, an A-factor-deficient mutant. *Microbiol.* 138: 1887–  
662 1892.
- 663 Tamura, K., Peterson, D., Peterson, N., Stecher, G., Nei, M., and Kumar, S. (2011) MEGA5:  
664 molecular evolutionary genetics analysis using maximum likelihood, evolutionary  
665 distance, and maximum parsimony methods. *Mol Biol Evol* 28: 2731–9.
- 666 Ueda, K., Kawai, S., Ogawa, H., Kiyama, A., Kubota, T., Kawanobe, H., and Beppu, T. (2000)  
667 Wide distribution of interspecific stimulatory events on antibiotic production and  
668 sporulation among *Streptomyces* species. *J Antibiot* 53: 979–982.
- 669 Whelan, S. and Goldman, N. (2001) A general empirical model of protein evolution derived  
670 from multiple protein families using a maximum-likelihood approach. *Mol Biol* 18: 691–  
671 9.
- 672 Xiao, X., Prinn, R.G., Simmonds, P.G., Steele, L.P., Novelli, P.C., Huang, J., Langenfelds, R.L.,  
673 O’Doherty, S., Krummel, P.B., Fraser, P.J., Porter, L.W., Weiss, R.F., Salameh, P. and  
674 Wang, R.H.J. (2007) Optimal estimation of the soil uptake rate of molecular hydrogen  
675 from AGAGE and other measurements, *J Geophys Res*, 112: 1-15.
- 676 Yonemura, S., Yokozawa, M., Kawashima, S., and Tsuruta, H. (2000) Model analysis of the  
677 influence of gas diffusivity in soil on CO and H<sub>2</sub> uptake. *Tellus B* 52: 919–933.

678

679 **Table and Figure Legends**

680 Table 1. H<sub>2</sub> oxidation rates weighted by biomass (final protein mass) for Harvard Forest  
681 Isolate (HFI) strains and strains from culture collections (*S. cattleya*, *S. griseoflavus*, *R. equi*) at  
682 typical atmospheric (~0.53 ppm) H<sub>2</sub> mole fractions. H<sub>2</sub> uptake affinity (K<sub>m</sub>), the maximum  
683 reaction rate (V<sub>max</sub>), and the minimum threshold for consumption are listed for each culture.

684

685 Table 2. Effect of physical disturbances of the aerial structure on H<sub>2</sub> oxidation rates in  
686 sporulated cultures of *Streptomyces* sp. HFI8. Gently rolling 4 mm diameter glass beads over  
687 culture lawns (Figure S5) reduced the observed H<sub>2</sub> uptake. The H<sub>2</sub> oxidation rates (the 5<sup>th</sup>  
688 column) in twelve whole cultures of strain HFI8 growing in serum vials on solid R2A medium  
689 were measured between 2 and 15 days after inoculation (the 2<sup>nd</sup> column). In samples 1-6, the  
690 aerial biomass was isolated from substrate biomass using glass beads to transfer aerial biomass to  
691 an empty, sterile vial. The amount of transferred biomass was measured by protein assay (the 4<sup>th</sup>  
692 column). We tested using different amounts (2.5 and 10g) of 4 mm diameter glass beads (the 3<sup>rd</sup>  
693 column). H<sub>2</sub> uptake is reported for the fraction of aerial biomass transferred to glass beads (the  
694 6<sup>th</sup> column) and for the fraction of the lawn remaining in the original vial in the medium (the 7<sup>th</sup>  
695 column) measured within 2-4 hours. In samples 7-12, all biomass was left in the original vial,  
696 and H<sub>2</sub> oxidation rates were measured before and after treatment with glass beads. The difference  
697 in uptake due to the procedure (the sum of the uptake rates reported in the 6<sup>th</sup> and the 7<sup>th</sup> column  
698 minus the uptake before transfer in the 5<sup>nd</sup> column) is reported in the 8<sup>th</sup> column.

699

700 Figure 1. High-resolution time series of H<sub>2</sub> uptake in three replicate cultures of  
701 *Streptomyces* sp. HFI8. The lettered arrows at various time points correspond to the micrographs  
702 of the life cycle shown in Figure S4: (A) the substrate mycelium, (B) the formation of aerial



703 hyphae and onset of sporulation, (C-H) cultures contain mainly spores. Enlarged inset shows the  
704 higher resolution measurements taken during the first four days. The detection limit (dashed  
705 lines) of  $\pm 0.24 \text{ nmol h}^{-1}$  is reported as the double standard deviation of four values measured in  
706 uninoculated control vials (black dots).

707

708 Figure 2. Consumption of  $\text{H}_2$  by *Rhodococcus equi* in liquid culture. (a)  $\text{H}_2$  oxidation  
709 rate, (b) cell biomass (protein concentration). All data are shown for three liquid culture  
710 replicates. The detection limit (dashed lines) is of  $\pm 0.12 \text{ nmol h}^{-1}$  and calculated as the double  
711 standard deviation of ten values measured in uninoculated control vials (black dots). Colored  
712 triangles show the results of concentration and dilution experiments. Cells in exponential phase  
713 were concentrated in either fresh TSB medium (green) or water (orange) to match protein  
714 concentrations in late exponential and stationary phase. Alternatively, cells from stationary phase  
715 were diluted in either fresh TSB medium (green) or water (orange) to protein concentrations  
716 similar to those in exponential phase cultures.

717

718 Table S1. The top database matches for strain HFI6 - HFI9 16S rRNA gene and *hhyL*  
719 nucleotide sequences indicate that the strains are *Streptomyces* spp. containing *hhyL* sequences.  
720 The GenBank accession number is listed for each deposited sequence. The results of NCBI  
721 Megablast BLAST search are listed for each sequence, where queries were made for the 16S  
722 rRNA sequences against the 16S rRNA gene sequence database and for the *hhyL* sequences  
723 against the entire nucleotide sequence database. The top match for each BLAST search is listed  
724 along with the total score, E value, and maximum identity of the match. Strain HFI6 - HFI9 16S  
725 rRNA gene sequences were 100% identical to several different strains of *Streptomyces* spp.

726 Strain HFI6 - HFI9 *hhyL* sequences are highly similar to published cultured and uncultured *hhyL*  
727 sequences, of which some were submitted to public databases as *hydB*-like genes, though the  
728 *hhyL* terminology has been more recently adopted (Constant et al., 2011b).

729

730 Figure S1. Photographs of *Streptomyces griseoflavus* Tu4000 and *Streptomyces* sp. HFI6  
731 - HFI9 soil isolate colonies on R2A medium plates. *S. griseoflavus* Tu4000 had the smooth and  
732 waxy appearance of a *bld* (bald) *Streptomyces* mutant, while strains HFI6 - HFI9 formed fuzzy  
733 colonies consistent with the presence of aerial hyphae. The pigmentation of strains HFI6 - HFI8  
734 was light pink and strain HFI9 was darker with a brown exudate secreted into the surrounding  
735 medium. HFI6 - HFI9 strains had the strong scent of geosmin, while *S. griseoflavus* Tu4000 did  
736 not.

737

738

739 Figure S2. Photomicrographs of *Streptomyces griseoflavus* Tu4000 and *Streptomyces* sp.  
740 HFI6 - HFI9 soil isolate cultures on R2A medium plates. The same samples are photographed in  
741 Figure S1. Only substrate mycelia are visible in the *S. griseoflavus* Tu4000 colony, while HFI6 -  
742 HFI9 strains had plentiful aerial hyphae.

743

744 Figure S3. Molecular phylogenetic analysis of *hhyL* sequences by the Maximum  
745 Likelihood method. The diversity of the high-affinity group 5 [NiFe]-hydrogenase (*hhyL*)  
746 sequences of the strains (bold) we tested for H<sub>2</sub> uptake (Table 1) are compared with *hhyL*  
747 sequences from the NCBI microbial genome database in this amino acid tree. The *hhyL*-  
748 containing *Streptomyces* sequences form two distinct clusters at a deep 99% bootstrap branch:

749 Cluster 1 and Cluster 2. Isolates that have been tested for H<sub>2</sub> uptake are marked to indicate  
750 whether (\*) or not (†) high-affinity H<sub>2</sub> uptake was observed. Culture collection strains  
751 investigated in this study were selected to broaden representation across the clusters and genera:  
752 *Streptomyces griseoflavus* Tu4000 (Cluster 1), *Rhodococcus equi* (*Actinobacterium*, Cluster 1),  
753 and *Streptomyces cattleya* (Cluster 2). Strains HFI6, HFI7, HFI8, and *S. griseoflavus* Tu4000  
754 *hhyL* are closely related to Cluster 1 *Streptomyces* spp. soil isolates that take up H<sub>2</sub> (summarized  
755 in Constant et al., 2011b), while strain HFI9 *hhyL* is more closely related to the *R. equi hhyL*.  
756 Cluster 2 *S. cattleya hhyL* is closely related to *Streptomyces* sp. AP1 *hhyL*, which also consumes  
757 H<sub>2</sub> (Constant et al., 2011b). Other culture collection strains that have been tested for H<sub>2</sub> uptake  
758 include *Ralstonia eutropha* H16 (Conrad et al., 1983b) and *Mycobacterium smegmatis* (King,  
759 2003). The evolutionary history was inferred by using the Maximum Likelihood method based  
760 on the Whelan and Goldman, 2010 model. The *hhyL* gene from an archaeon *Sulfolobus*  
761 *islandicus* HVE10/4 was used as the outgroup. The bootstrap values are shown next to the  
762 branches. Initial tree(s) for the heuristic search were obtained automatically by applying  
763 Neighbor-Join and BioNJ algorithms to a matrix of pairwise distances estimated using a WAG  
764 model, and then selecting the topology with superior log likelihood value. A discrete Gamma  
765 distribution was used to model evolutionary rate differences among sites (5 categories (+G,  
766 parameter = 1.2590)). The tree is drawn to scale, with branch lengths measured in the number of  
767 substitutions per site. The analysis involved 58 amino acid sequences. There were a total of 427  
768 positions in the final dataset. Evolutionary analyses were conducted in MEGA5 (Tamura et al.,  
769 2011).  
770

771           Figure S4. Microscopic observations of the development of *Streptomyces* sp. HFI8 show  
772 that strain HFI8 underwent the full lifecycle from spore to spore in less than 1.8 days, after  
773 which nearly all the viable cells existed as spores. Each panel shows a representative micrograph  
774 of the culture taken on a different day after the inoculation. Image A shows the substrate  
775 mycelium that grows after the germination of inoculated spores. By day 1.8 (B), septated aerial  
776 hyphae (punctuated tubular branches) and fully formed spores (round cells) are present. Mainly  
777 spores are present from day 2.9 to 22 (C-H) and the same persists until day 44 (not shown).  
778

779           Figure S5. Photograph of serum vials during the aerial biomass removal experiments  
780 (Table 2, Samples 1-6) illustrates the separation of the aerial hyphae and spores from the  
781 substrate mycelium: a) vial containing an *whole* intact strain HFI8 culture (Table 2, column 5);  
782 b) vial from which the aerial biomass had been isolated using glass beads leaving behind the  
783 remaining *substrate* mycelium (Table 2, column 7); and c) vial containing the isolated *aerial*  
784 biomass on the surface of the glass beads (Table 2, column 6). In some samples, glass beads  
785 were rolled on the whole colony surface (a) and were left in the same vial with no biomass  
786 transfer (Table 2, Samples 7-12).  
787

788           Figure S6. Scatter plot of the initial H<sub>2</sub> oxidation rate versus the reduction in H<sub>2</sub> uptake  
789 by *Streptomyces* sp. HFI8 during the glass bead procedure (Table 2; 5<sup>th</sup> and 8<sup>th</sup> columns). The  
790 larger the initial H<sub>2</sub> oxidation rate, the larger percentage reduction by the glass beads ( $R^2=0.93$ ),  
791 regardless of culture age or the amount of glass beads used for transfer.  
792

793           Figure S7: Determination of H<sub>2</sub> uptake kinetic parameters by the Lineweaver-Burk (LB)  
794 and Eadie-Hofstee (EH) methods for *Streptomyces* sp. HFI8. The H<sub>2</sub> uptake rate (V) nmol h<sup>-1</sup>  
795 and initial H<sub>2</sub> concentration (S) in ppm are used to generate the LB plot as 1/V versus 1/S and  
796 EH as V versus V/S. K<sub>m</sub> was determined from the LB plot as the K<sub>m</sub> = -1 / x-intercept (38 ppm)  
797 and V<sub>max</sub> as V<sub>max</sub> = 1/y-intercept (30 μmol min<sup>-1</sup> g<sup>-1</sup>). K<sub>m</sub> was determined from the EH plot as K<sub>m</sub>  
798 = -slope (22 ppm). K<sub>m</sub> and V<sub>max</sub> values were reported for a given strain only if the LB and EH  
799 K<sub>m</sub> values methods agreed within 50%`  
800

Table 1. H<sub>2</sub> oxidation rates weighted by biomass (final protein mass) for Harvard Forest Isolate (HFI) strains and strains from culture collections (*S. cattleya*, *S. griseoflavus*, *R. equi*) at typical atmospheric (~0.53 ppm) H<sub>2</sub> mole fractions. H<sub>2</sub> uptake affinity (K<sub>m</sub>), the maximum reaction rate (V<sub>max</sub>), and the minimum threshold for consumption are listed for each culture.

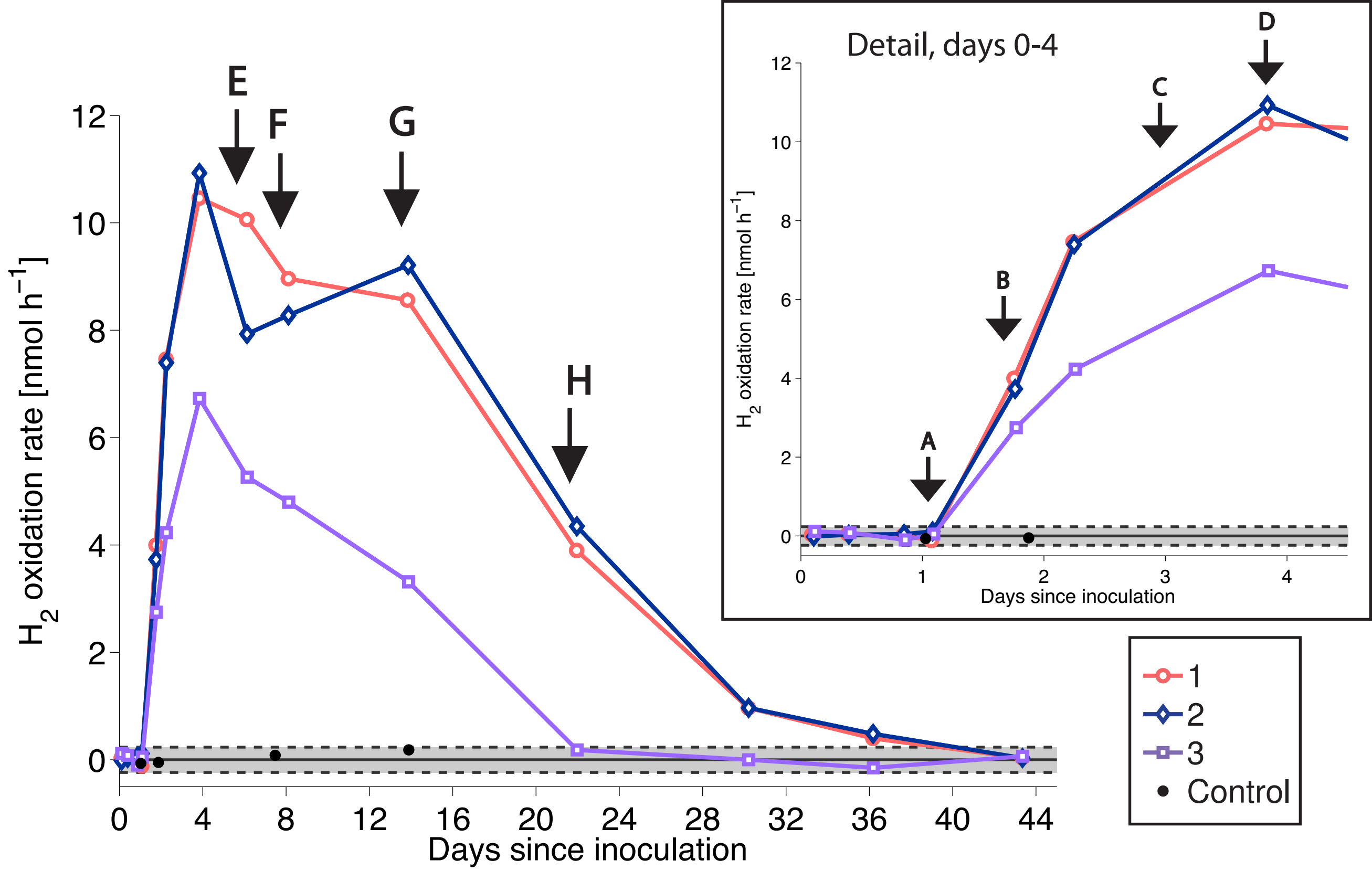
Strain	H <sub>2</sub> oxidation rate [nmol min <sup>-1</sup> g <sup>-1</sup> ]	K <sub>m</sub> * [ppm]	V <sub>max</sub> * [μmol min <sup>-1</sup> g <sup>-1</sup> ]	Threshold [ppm]
<i>Streptomyces</i> sp. HFI6	780	80	180	<0.15
<i>Streptomyces</i> sp. HFI7	420	60	78	<0.12
<i>Streptomyces</i> sp. HFI8	240	40	30	<0.15
<i>Streptomyces</i> sp. HFI9	100	40	14	<0.12
<i>Streptomyces griseoflavus</i> Tu4000	0	-	-	-
<i>Streptomyces cattleya</i>	130	**	**	<0.45
<i>Rhodococcus equi</i>	10	**	**	<0.30

\* Determined by the Lineweaver-Burke method over a 0-35 ppm H<sub>2</sub> range, which is less precise than the non-inverse approach, but avoids interference by low-affinity hydrogenases.

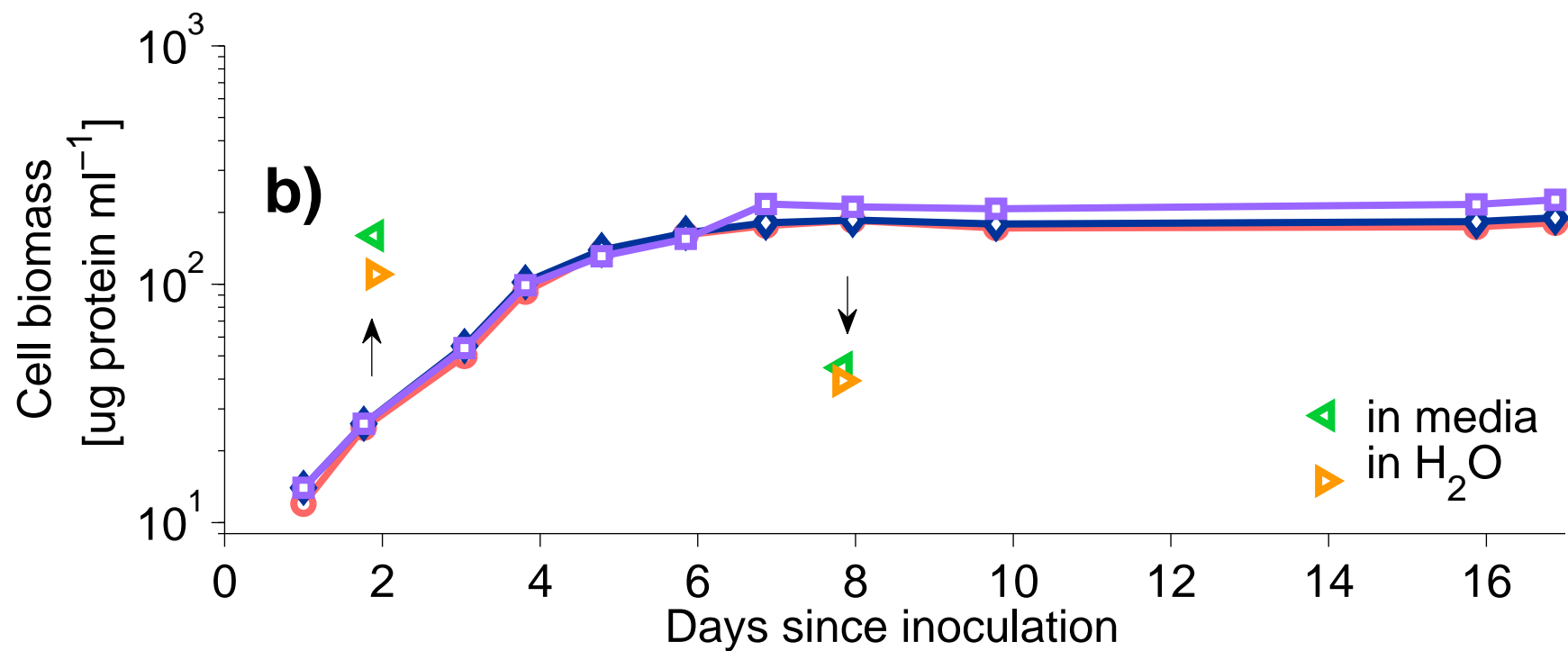
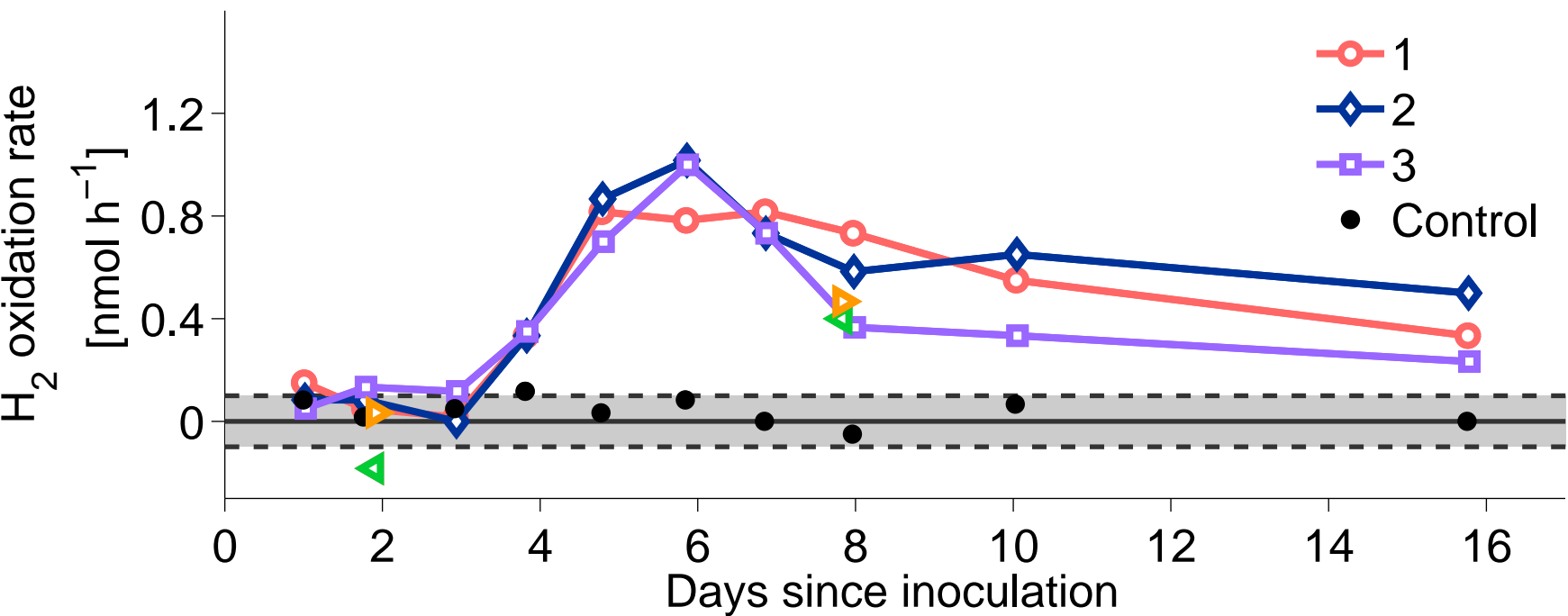
\*\* Kinetic parameters determination did not pass quality check (Experimental Procedures).

Table 2. Effect of physical disturbances of the aerial structure on H<sub>2</sub> oxidation rates in sporulated cultures of *Streptomyces* sp. HFI8. Gently rolling 4 mm diameter glass beads over culture lawns (Figure S5) reduced the observed H<sub>2</sub> uptake. The H<sub>2</sub> oxidation rates (the 5<sup>th</sup> column) in twelve whole cultures of strain HFI8 growing in serum vials on solid R2A medium were measured between 2 and 15 days after inoculation (the 2<sup>nd</sup> column). In samples 1-6, the aerial biomass was isolated from substrate biomass using glass beads to transfer aerial biomass to an empty, sterile vial. The amount of transferred biomass was measured by protein assay (the 4<sup>th</sup> column). We tested using different amounts (2.5 and 10g) of 4 mm diameter glass beads (the 3<sup>rd</sup> column). H<sub>2</sub> uptake is reported for the fraction of aerial biomass transferred to glass beads (the 6<sup>th</sup> column) and for the fraction of the lawn remaining in the original vial in the medium (the 7<sup>th</sup> column) measured within 2-4 hours. In samples 7-12, all biomass was left in the original vial, and H<sub>2</sub> oxidation rates were measured before and after treatment with glass beads. The difference in uptake due to the procedure (the sum of the uptake rates reported in the 6<sup>th</sup> and the 7<sup>th</sup> column minus the uptake before transfer in the 5<sup>nd</sup> column) is reported in the 8<sup>th</sup> column.

ID	Day	Beads [g]	Aerial biomass [mg]	H <sub>2</sub> oxidation rate [nmol h <sup>-1</sup> ]			
				Whole	Aerial + glass beads	Substrate	Change in net uptake (%)
1	2	10	na	4.1	0.6	1.5	-1.9 (-48%)
2	8	10	0.3	6.8	0.3	2.9	-3.6 (-52%)
3	15	10	0.1	6.9	0.3	1.7	-4.9 (-71%)
4	9	2.5	1.5	3.6	0.1	2.1	-1.4 (-40%)
5	9	5	0.6	3.8	0.1	2.2	-1.4 (-37%)
6	9	10	1.1	3.8	0.1	2.1	-1.6 (-43%)
				Whole	Whole + glass beads		
7	9	10	na	2.2	1.3		-0.9 (-41%)
8	9	10	na	2.8	2.1		-0.7 (-25%)
9	9	10	na	2.4	1.5		-0.9 (-38%)
10	9	10	na	1.5	2.0		-0.3 (-20%)
11	9	10	na	2.4	2.0		-0.4 (-18%)
12	9	10	na	2.2	1.9		-0.3 (-13%)



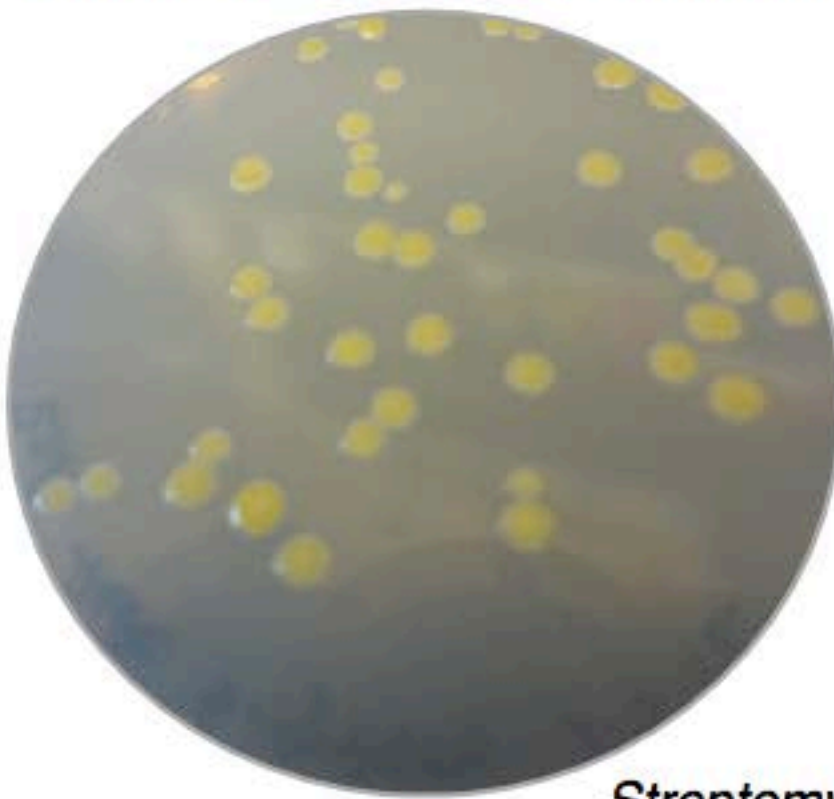




1 Table S1. The top database matches for strain HFI6 - HFI9 16S rRNA gene and *hhyL* nucleotide sequences indicate that the strains are  
2 *Streptomyces* spp. containing *hhyL* sequences. The GenBank accession number is listed for each deposited sequence. The results of  
3 NCBI Megablast BLAST search are listed for each sequence, where queries were made for the 16S rRNA sequences against the 16S  
4 rRNA gene sequence database and for the *hhyL* sequences against the entire nucleotide sequence database. The top match for each  
5 BLAST search is listed along with the total score, E value, and maximum identity of the match. Strain HFI6 - HFI9 16S rRNA gene  
6 sequences were 100% identical to several different strains of *Streptomyces* spp. Strain HFI6 - HFI9 *hhyL* sequences are highly similar  
7 to published cultured and uncultured *hhyL* sequences, of which some were submitted to public databases as *hydB*-like genes, though  
8 the *hhyL* terminology has been more recently adopted (Constant et al., 2011b).  
9

Strain	Gene	Nucleotide sequence	BLAST results				
			Accession number	Top database match (accession number)	Total Score	E value	Max ident
HFI6	16S rRNA	<a href="#">KC661265</a>		<i>Streptomyces lavendulae</i> subsp. <i>lavendulae</i> strain NBRC 12344 ( <a href="#">AB184081.2</a> )	2532	0.0	100%
HFI7	16S rRNA	<a href="#">KC661266</a>		<i>Streptomyces roseochromogenus</i> strain MJM9261 ( <a href="#">GU296744.1</a> )	2532	0.0	100%
HFI8	16S rRNA	<a href="#">KF444073</a>		<i>Streptomyces roseochromogenus</i> strain MJM9261 ( <a href="#">GU296744.1</a> )	2532	0.0	100%
HFI9	16S rRNA	<a href="#">KF444074</a>		<i>Streptomyces sanglieri</i> strain NBRC 100784 ( <a href="#">NR_041417.1</a> )	2521	0.0	100%
HFI6	<i>hhyL</i>	<a href="#">KC661267</a>		<i>Streptomyces</i> sp. MP1 NiFe-hydrogenase large subunit ( <i>hydB</i> ) gene ( <a href="#">GQ867040.1</a> )	1838	0.0	95%
HFI7	<i>hhyL</i>	<a href="#">KC661268</a>		<i>Streptomyces</i> sp. MP1 NiFe-hydrogenase large subunit ( <i>hydB</i> ) gene ( <a href="#">GQ867040.1</a> )	1866	0.0	96%
HFI8	<i>hhyL</i>	<a href="#">KC661269</a>		<i>Streptomyces</i> sp. MP1 NiFe-hydrogenase large subunit ( <i>hydB</i> ) gene ( <a href="#">GQ867040.1</a> )	1432	0.0	97%
HFI9	<i>hhyL</i>	<a href="#">KC661270</a>		<i>Streptomyces</i> sp. S9n30 partial <i>hhyL</i> gene for [NiFe]-hydrogenase ( <a href="#">HF677116.1</a> )	2207	0.0	99%

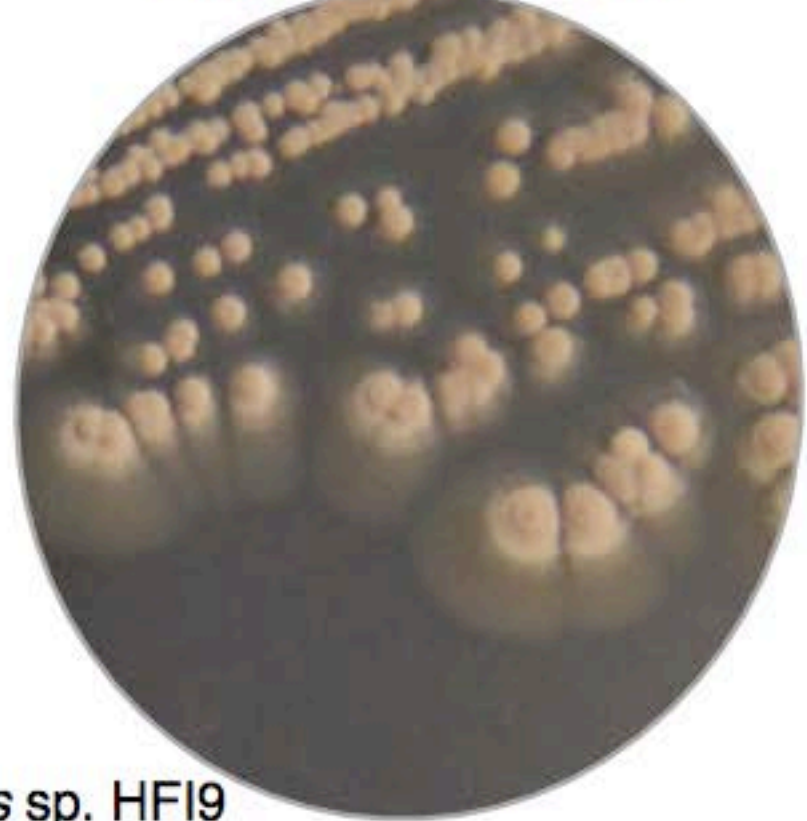
*Streptomyces griseoflavus* Tu4000



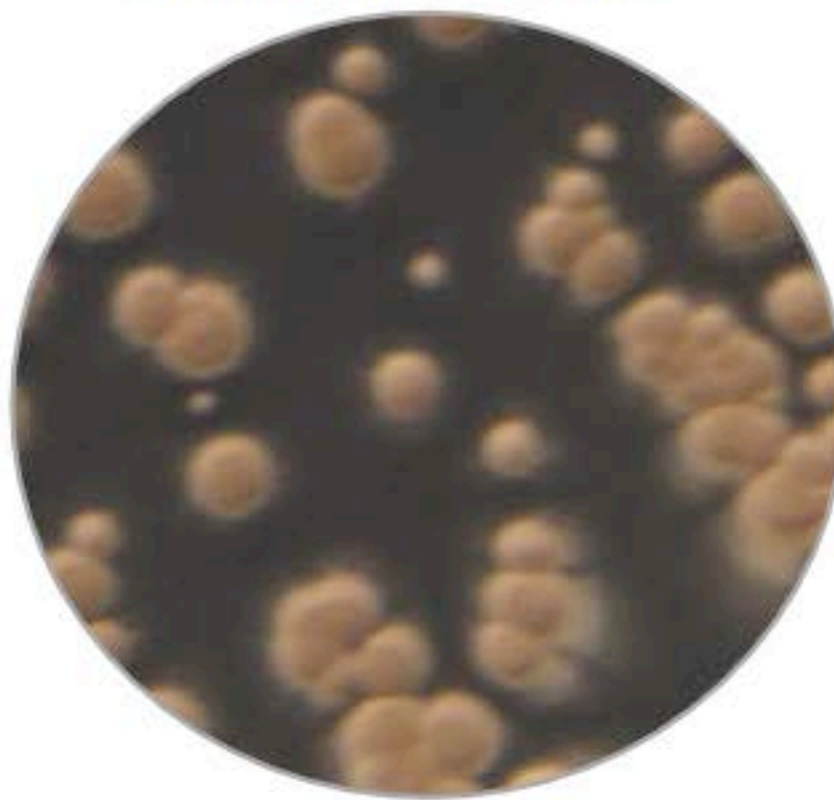
*Streptomyces* sp. HF16



*Streptomyces* sp. HF17



*Streptomyces* sp. HF18

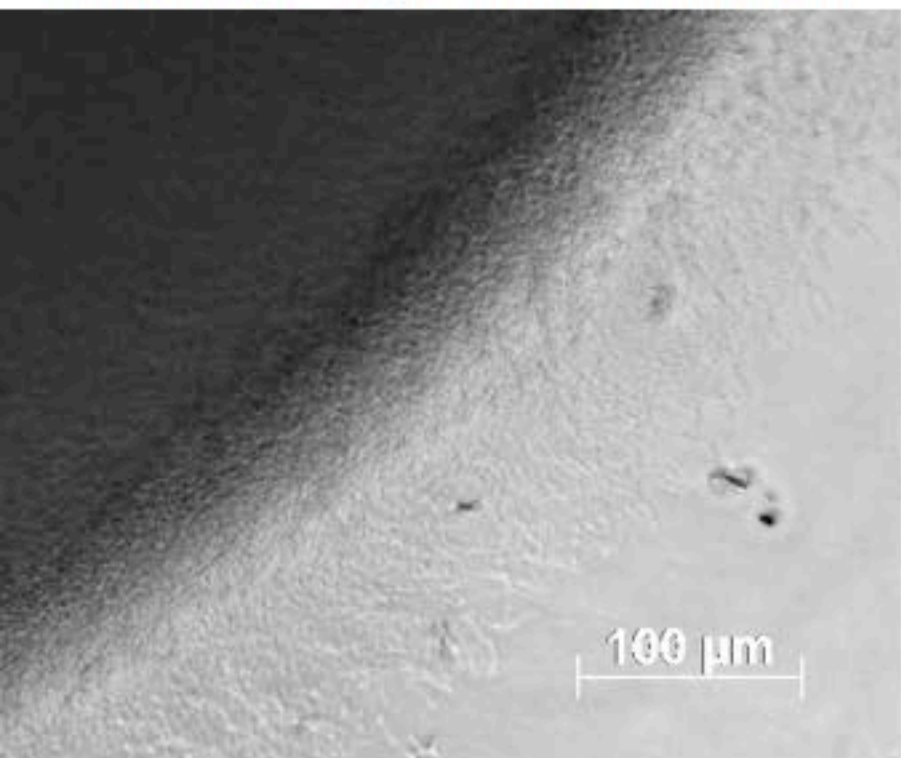


*Streptomyces* sp. HF19

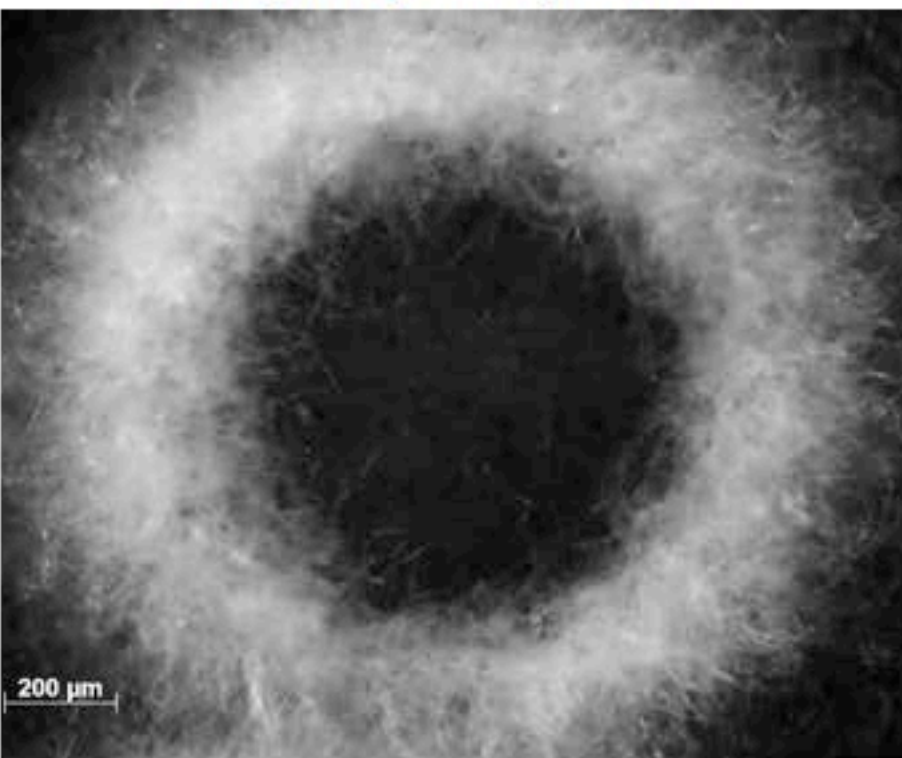




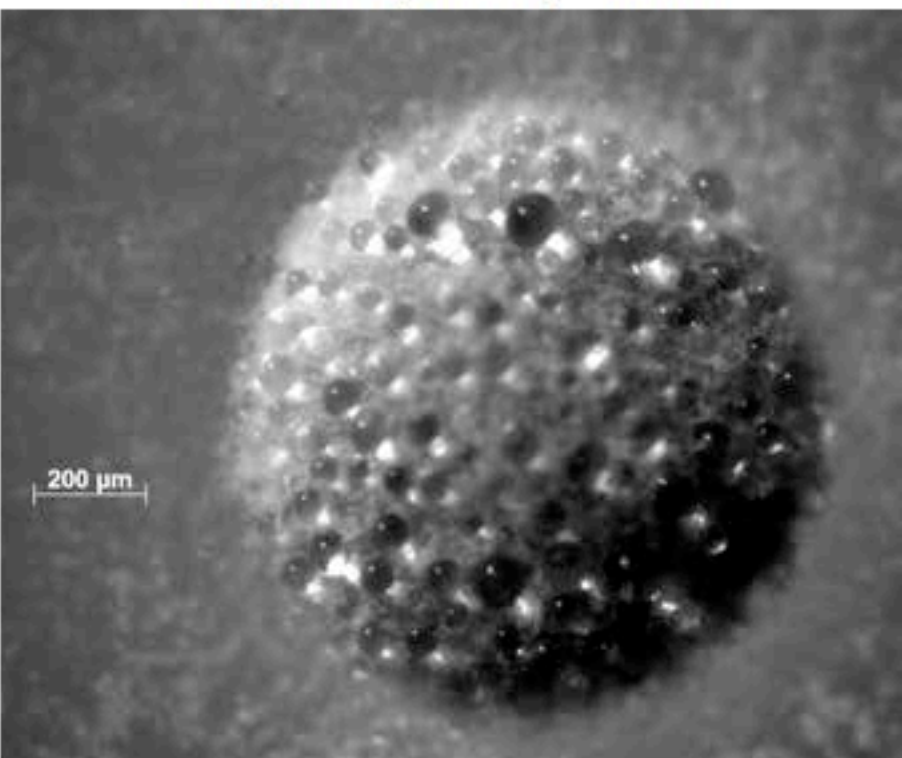
*Streptomyces griseoflavus* Tu4000



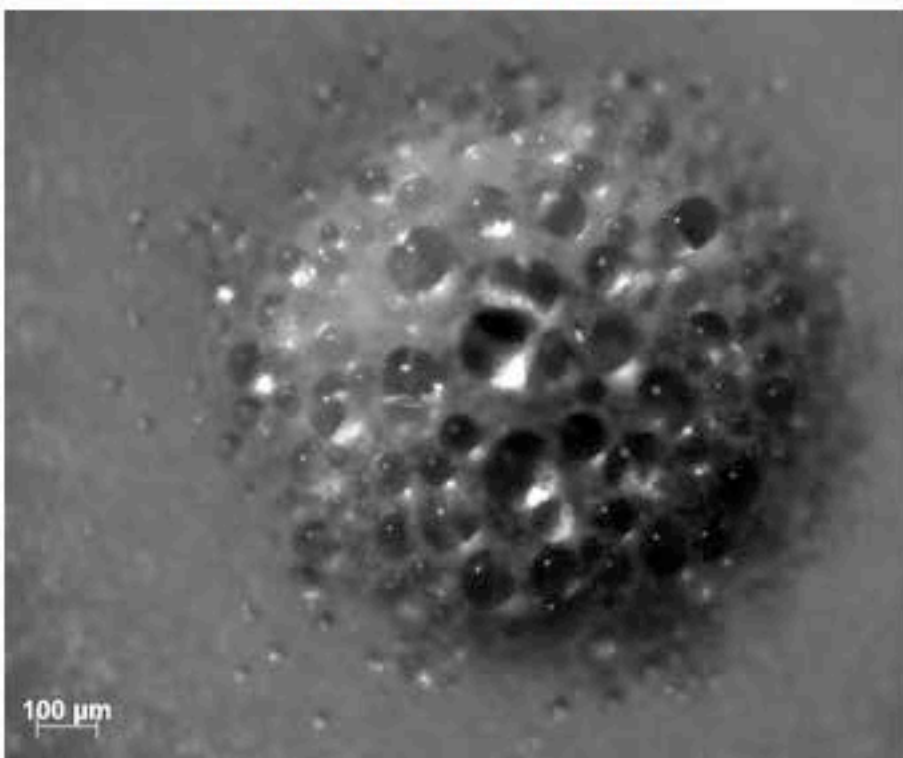
*Streptomyces* sp. HF16



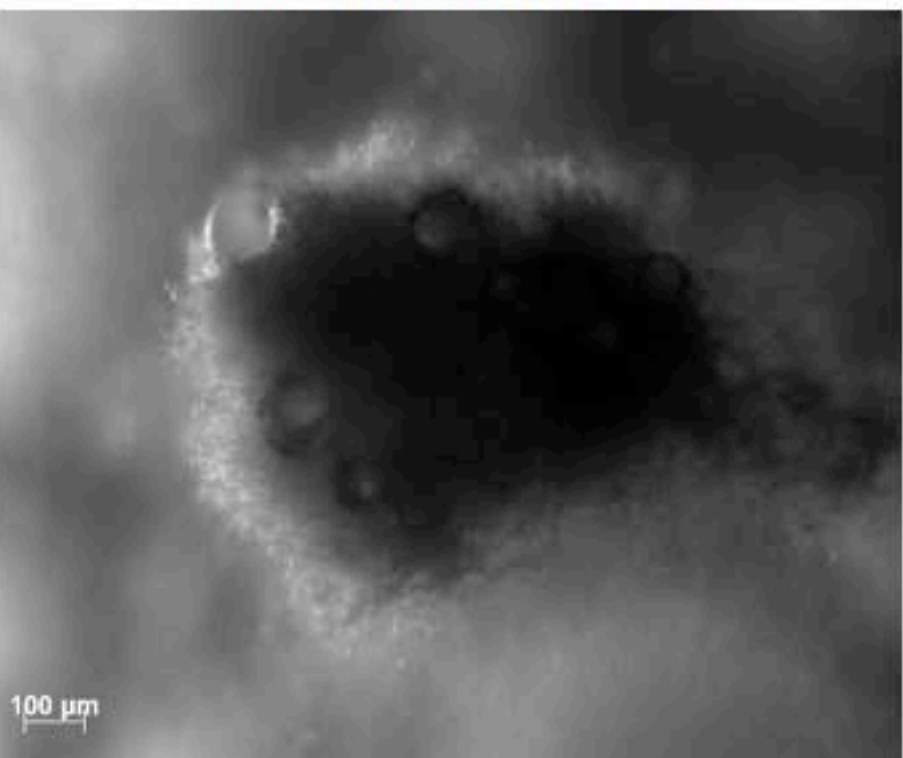
*Streptomyces* sp. HF17

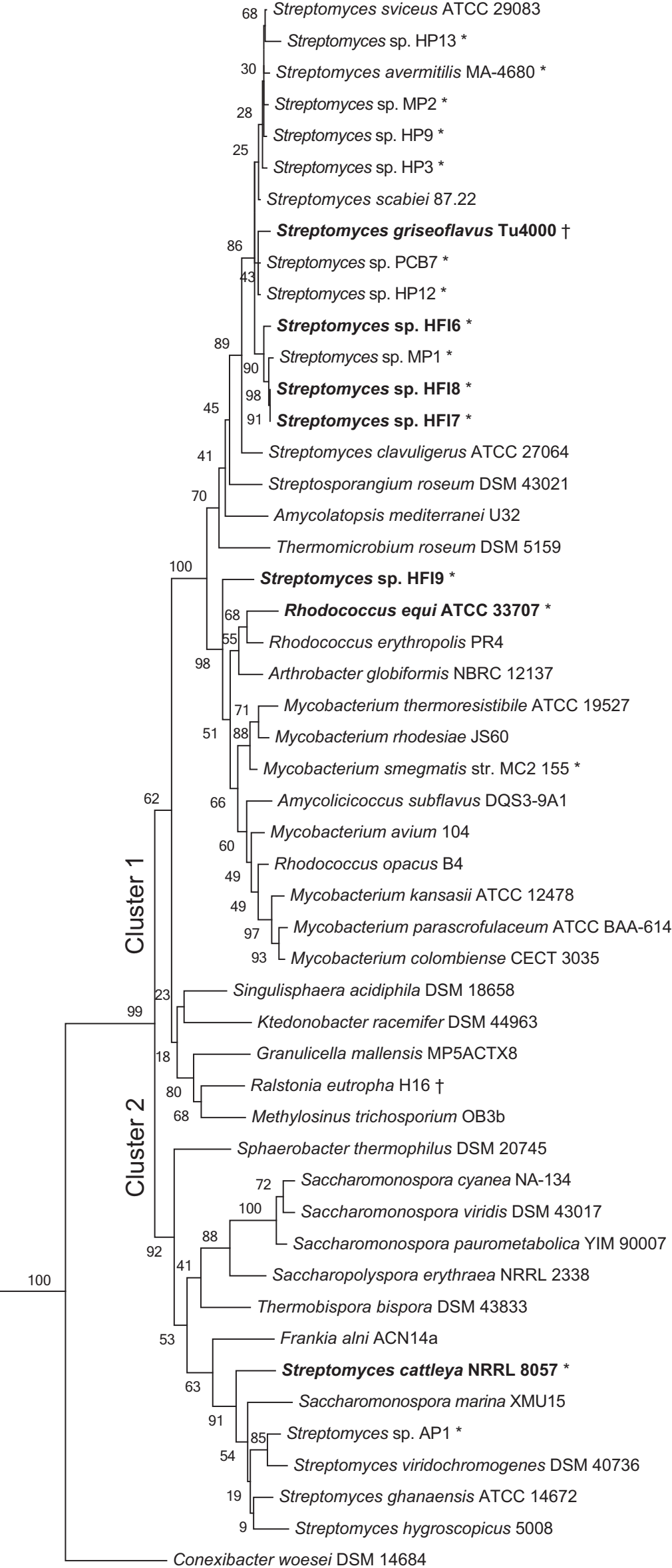


*Streptomyces* sp. HF18



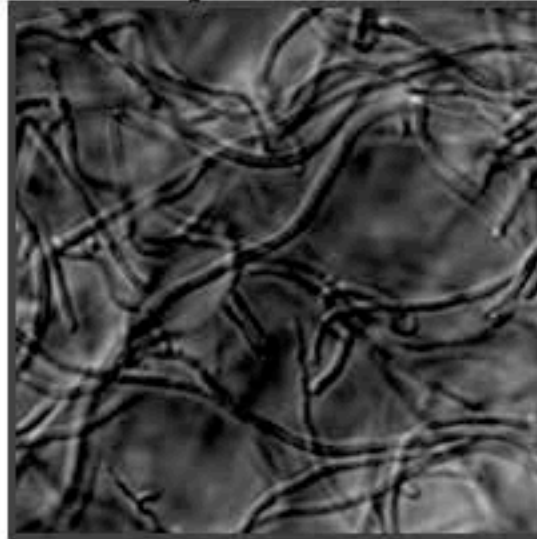
*Streptomyces* sp. HF19



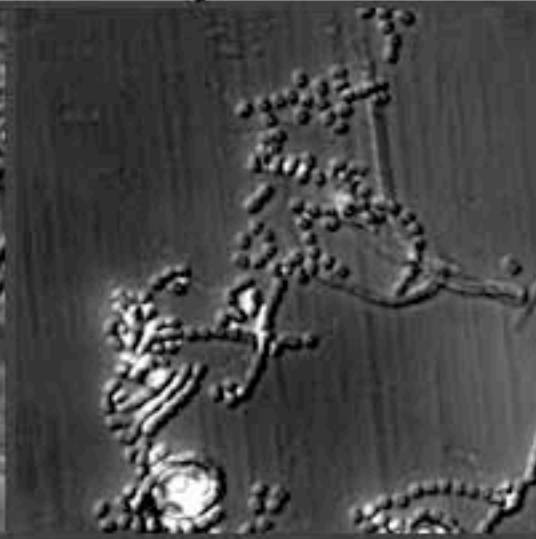


# *Streptomyces* sp. HF18

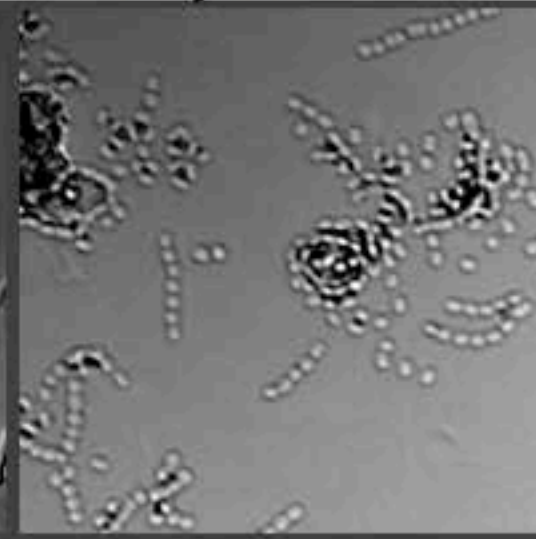
B : Day 1.1



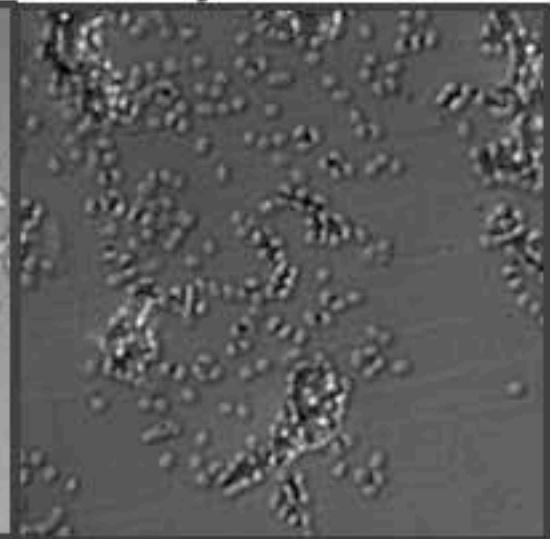
C : Day 1.8



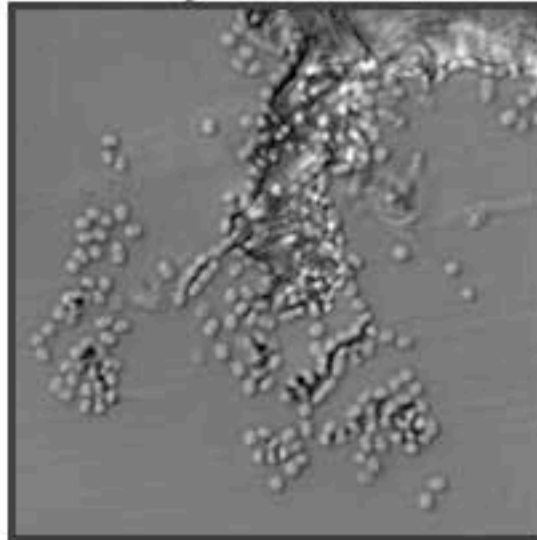
D : Day 2.9



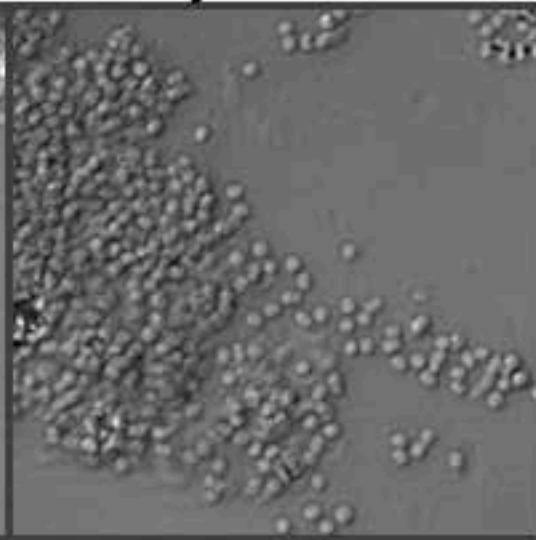
E : Day 3.8



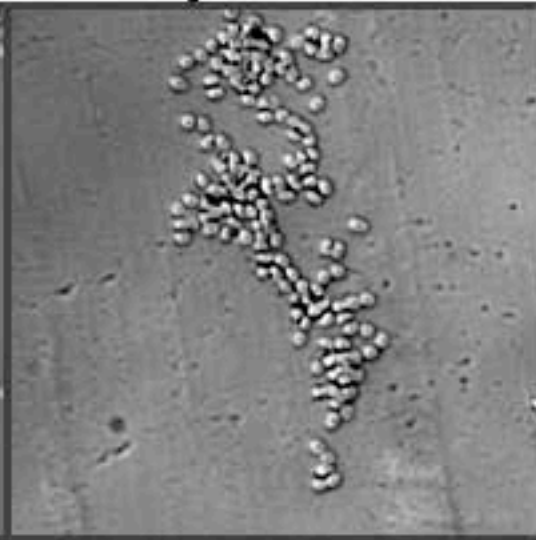
F : Day 6.1



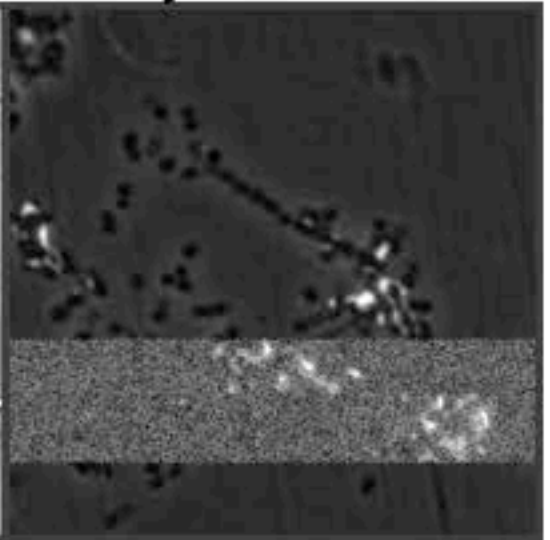
G : Day 8.1



H : Day 13.8



I : Day 22.0



10  $\mu$ m



a

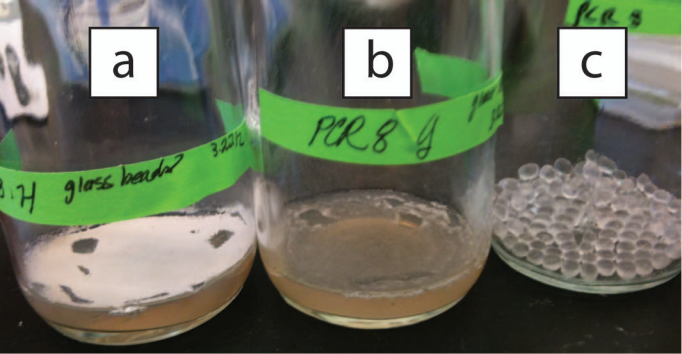
H. H glass beads 3.22 μ

b

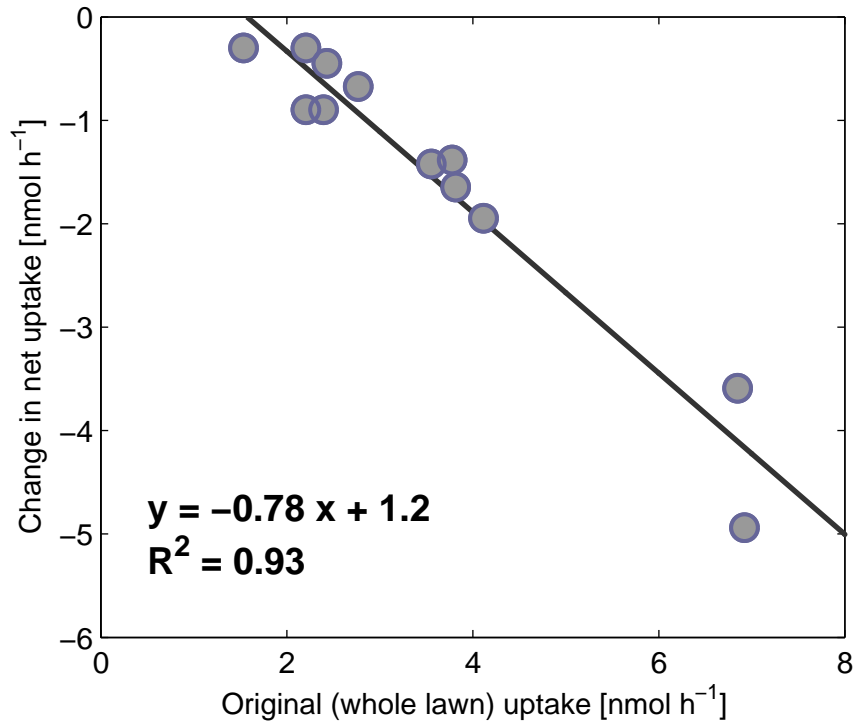
PCR 8 g

c

PCR 8 g



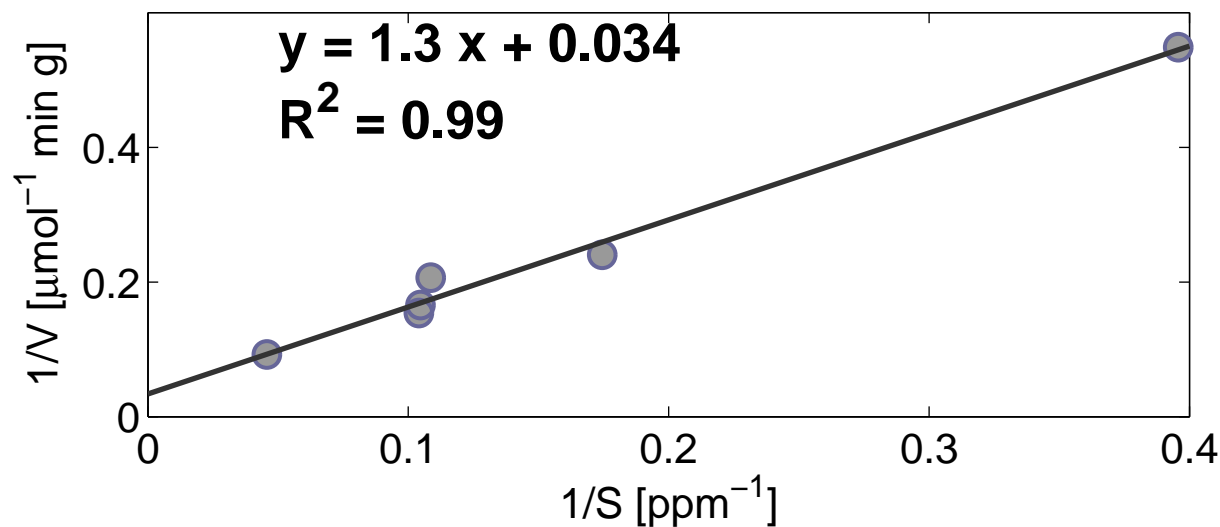
Loss in H<sub>2</sub> uptake by disturbance depends on original uptake





# Kinetic Parameter Determination for Strain HFI8

Lineweaver-Burk Plot



Eadie-Hofstee Plot

